

Spring 2019

The influence of surface reinforcement on concrete failure under shear loading

James Buban

Iowa State University, jabuban@iastate.edu

Follow this and additional works at: <https://lib.dr.iastate.edu/creativecomponents>



Part of the [Structural Engineering Commons](#)

Recommended Citation

Buban, James, "The influence of surface reinforcement on concrete failure under shear loading" (2019).
Creative Components. 145.

<https://lib.dr.iastate.edu/creativecomponents/145>

This Creative Component is brought to you for free and open access by the Iowa State University Capstones, Theses and Dissertations at Iowa State University Digital Repository. It has been accepted for inclusion in Creative Components by an authorized administrator of Iowa State University Digital Repository. For more information, please contact digirep@iastate.edu.

The influence of surface reinforcement on concrete failure under shear loading

by

James Buban

A Creative Component submitted to the graduate faculty
in partial fulfillment of the requirements for the degree of

MASTER OF SCIENCE

Major: Civil Engineering (Structural Engineering)

Program of Study Committee:
Dr. An Chen, Major Professor
Dr. Jiehua Shen
Dr. Bora Cetin

Iowa State University

Ames, Iowa

2019

Copyright © James Buban, 2019. All rights reserved.

TABLE OF CONTENTS

LIST OF FIGURES	i
LIST OF TABLES	iv
ABSTRACT.....	v
CHAPTER 1: INTRODUCTION	1
1.1 Background	1
1.1.1 Necessity of Cost-Effective Improvements in Construction Industry	1
1.1.2 Uses and Importance of Fastenings to Concrete.....	1
1.1.3 History of the Approaches used to Determine Shear Capacity of Concrete.....	3
1.1.4 Current Method used to Determine Concrete Breakout in Shear	6
1.1.5 Size Effect of Anchor Bolts	9
1.1.6 Current Standard Definition of Supplemental Reinforcement.....	11
1.1.7 Sizing and Capacity of Shear Reinforcement	18
1.2 Problem Statement.....	20
CHAPTER 2: FINITE ELEMENT ANALYSIS	21
2.1 Introduction.....	21
2.2 Model Design.....	22
2.2.1 Model Geometry	22
2.2.2 Model Properties.....	25
2.3 Finite Element Analysis Results	28
2.3.2 Control Model with Reinforcement 4in Spacing (Model 2, Figure 2.10)	30
2.3.3 Experimental Model with Reinforcement 6in Spacing (Model 3, Figure 2.13)	31
2.3.4 Experimental Model with Reinforcement 8in Spacing (Model 4, Figure 2.16)	33
2.3.5 Force vs. Displacement Results.....	35
CHAPTER 3: CONCLUSION	36
3.1 Overall Conclusion	36
3.1.1 Recommended Modification.....	38
3.2 Field Application	39
3.3 Future Studies	39
CHAPTER 4: REFERENCES	41
CHAPTER 5: APPENDIX A. HAND CALCULATIONS	43

LIST OF FIGURES

Figure 1.1 - ACI 349-85 (Projected Area of Failure Cone).....	3
Figure 1.2 - Concrete Failure Surface with Reductions for Edges	4
Figure 1.3 - Idealized Concrete Failure Surface	4
Figure 1.4 - Embedment Depth and Failure Load Curve.....	10
Figure 1.5 - Lateral Distribution of Longitudinal and Edge Reinforcement – CEB	11
Figure 1.6 - The effect of reinforcement on load-bearing behavior of single anchors close to an edge – (Eligehausen 2006b).....	12
Figure 1.7 - Lateral Distribution of Longitudinal and Edge Reinforcement - ACI 318-14.....	13
Figure 1.8 - Hairpin Reinforcement Details tested	14
Figure 1.9 - ASCE Stirrup Reinforcement Detail using STM.....	15
Figure 1.10 - Development Length of Suppl. Reinf. using Hairpins ACI 318-14.....	17
Figure 1.11 - Development Length for Hairpin Reinforcement beyond failure surface - CEB ...	17
Figure 1.12 - Stirrup Reinforcement Development Length - ACC	17
Figure 2.1 - Dimensions of Steel Anchor; All Model.....	22
Figure 2.2 - Dimensions of Concrete Block; All Models	23
Figure 2.3 - Dimensions of Stirrup Design used Throughout Study	24
Figure 2.4 - Edge Reinforcement Dimensions used Throughout Study	24
Figure 2.5 - Boundary Condition and Displacement Control (same for all models).....	25
Figure 2.6 - Von Mises Stress for Steel Anchor (Model 2 results).....	27
Figure 2.7 - Concrete Tensile Damage Parameter for Model 1	28
Figure 2.8 - Failure Surface predicted using the CCD Method	28
Figure 2.9 - Concrete Compressive Damage Parameter for Model 1	29
Figure 2.10 - Diagram of Model 2	30
Figure 2.11 - Concrete Tensile Damage Parameter for Model 2	30
Figure 2.12 - Von Mises Stress in No. 5 Stirrups (left), Max stress on Single Stirrup (right) for Model 2	31
Figure 2.13 - Diagram of Model 3	31
Figure 2.14 - Concrete Tensile Damage Parameter for Model 3	32
Figure 2.15 - Von Mises Stress in No. 5 Stirrups (left), Max stress on Single Stirrup (right) for Model 3	33

Figure 2.16 - Diagram of Model 4	33
Figure 2.17 - Von Mises Stress in No. 5 Stirrups (left), Max stress on Single Stirrup (right) for Model 4	34
Figure 2.17 - Concrete Tensile Damage Parameter for Model 4	34
Figure 2.19 - Force vs Displacement Results from FEA	35

LIST OF TABLES

Table 1.1 - Shear Breakout Equations used in ACI 318-14.....	6
Table 1.2. Shear Breakout Equations used in ACI 349-85	6
Table 1.3. Shear Breakout Equations used in CEB – “Design of Fastenings”	6
Table 1.4. Shear Breakout Equations proposed for CCD Approach	7
Table 1.5. Shear Breakout Equations used in “Anchorage in Concrete Construction”	7
Table 1.6 - Development Length and Hanger Reinforcement Capacity.....	16
Table 1.7 - Shear Strength of Supplemental Reinforcement	19
Table 2.1 - Concrete Compressive Damage Properties and Parameter adjusted for $f_c' = 4,000$ psi (Zhang 2018).....	26
Table 2.2 - Concrete Tensile Damage Properties and Parameter adjusted for $f_c' = 4,000$ psi (Zhang 2018).....	26
Table 2.3 - Summary of Peak Loads and Calculated anticipated Loads	35

ABSTRACT

Recently, construction costs have been at a global high – paired with increased global demand, rise in cost of material and limited skilled labor – it has become of utmost paramount to determine the solutions in the Civil Engineering industry to accommodate these changes and relieve these costs. Fastening to concrete has been important part of the construction industry for many years. Several standards have adopted a form of determining the strength of concrete breakout such as: ACI 318, ACI 349, or European code “Design of Fastenings in Concrete.” Many of these codes still reference testing and use equations that were developed in the early 1990’s. As technology in construction moves forward, so must the codes we use to design these new structures. Therefore, this study will evaluate whether the code is too conservative and can be expanded upon. Through the use of an FEA program, the effectiveness of shear anchor reinforcement is investigated. The load-bearing capacity is currently limited to three specific conditions: 1) No reinforcement present, 2) Edge reinforcement present, and 3) Edge reinforcement and stirrups spaced at 4in max. There are significant gaps in between these situations. Expanding condition 3) to include larger spacing would greatly benefit designers and laborers. Finite Element Analysis models will be run with 4 in, 6 in, and 8 in spacing between shear reinforcement stirrups. Peak loads will be extracted from each data and analyzed. Based on comparisons with the results, FE and calculations, recommendations are provided on the modification of existing code equations to expand to more conditions.

CHAPTER 1: INTRODUCTION

1.1 Background

1.1.1 Necessity of Cost-Effective Improvements in Construction Industry

Historically, the price of hot-rolled steel has fluctuated with the season; overall the industry has seen a steady decline in steel pricing in the last decade, costing approximately 630.49 USD/MT (US dollar per metric ton) in 2013 to 380 USD/MT in February 2016. However, in more recent history the price of steel has climbed to 833.11 USD/MT in 2018 (Focus Economics, 2019). According the World Steel Association, global steel demand is forecasted to grow by 1.8% in 2018 & 0.7% in 2019 (General Steel, 2019). A rise in demand may very well drive projected steel prices even higher. In addition to increased material costs, recent industrywide surveys have indicated that skilled labor wages will continue to rise at a steady pace due to significant shortage of qualified craft workers. According to the Labor Statistics Bureau, in 2016 more than 200,000 construction positions remained unfilled. This is an 81% increase from the previous two years. A significantly high percentage that results in higher labor wage costs and hinders the development of the industry (Pearman, 2018). Given these major factors, cost of construction will continue to escalate – leading to a push for more cost-effective designs. An area for cost reduction may be found in adjusting the design of concrete fasteners.

1.1.2 Uses and Importance of Fastenings to Concrete

Concrete fasteners come in a large range of shapes, sizes, and applications such as: embed plates with welded studs cast into the structure; post-installed wedge anchors used to secure a piece of machinery to a concrete slab, or a drilled and epoxy rod used to attach a precast architectural detail to the face a bridge pier. Fasteners, referred to as anchors, are defined as

“steel elements either cast into concrete or post-installed into a hardened concrete member and used to transmit applied loads to the concrete” (ACI 318-11). The quantity and arrangement of the anchor(s) is to be decided by the designer. Many factors need to be considered when designing the anchorage. Assuming that the steel itself has sufficient strength to resist the applied loads, the next failure mode is the portion of concrete affected by the transmittal of the loads. Similar to other structural connections, the clear distance of the fastener relative to adjacent edges or discontinuities will greatly affect the capacity of the connection. In the case of anchorage in concrete, the location of the anchor relative to free edges or openings will dictate how much load the concrete can resist. Other factors influencing capacity, such as: load distribution, spacing and embedment depth are also considered in the overall capacity of an anchor(s).

Cast-in-place anchors are becoming a prominent method used to make many different types of structural connections. Engineers are always trying to take full advantage of a structural connection and make the most economical and safe design possible. But the construction industry today is using these same anchorage devices to resist larger loads due to advancements in member design. Previous designs for anchorage devices are no longer adequate to support the increased demand imposed by the member. Anchorage in concrete construction must continue to develop in order to keep pace with the increased demand from the structural system, as well as, broaden the applications in which it can be used.

1.1.3 History of the Approaches used to Determine Shear Capacity of Concrete

The behavior of cast-in-place headed stud anchors have been tested and analyzed for many years. Up to and including most the 1980's, fastenings in concrete were designed to be limited by the steel itself. According to ACI 349-85 "Code Requirements for Nuclear Safety Related Concrete Structures", brittle failure of concrete was not allowed to govern the overall ductile steel failure strength of the connection regardless of loading. *"Bolts, studs, or bars shall meet the requirements of B.5.1.1. The minimum edge distance, m , for shear loading toward a free edge shall be such that the concrete design strength (based on a uniform tensile stress equal to $4\phi\sqrt{f'_c}$, acting on an effective area defined by projecting a 45° half-cone to the free surface from the centerline of the tensile stress component at the shearing place) exceeds the ultimate shear strength of the bolts, studs, or bars, (based on f_{ut}),"* (ACI 349-85). Ignoring the strength of concrete required that anchors have deeper embedment and larger edge distances to satisfy code. Under tension and shear, the concrete failure is governed by a cone formed at a 45° relative to the direction of force with uniform stress equal to $4\phi\sqrt{f'_c}$ over the projected failure surface. Reductions in the projected area are made by accounting for free edges and overlapping cones (See Figure 1.1). This methodology was the foundation on which anchor design was built on.

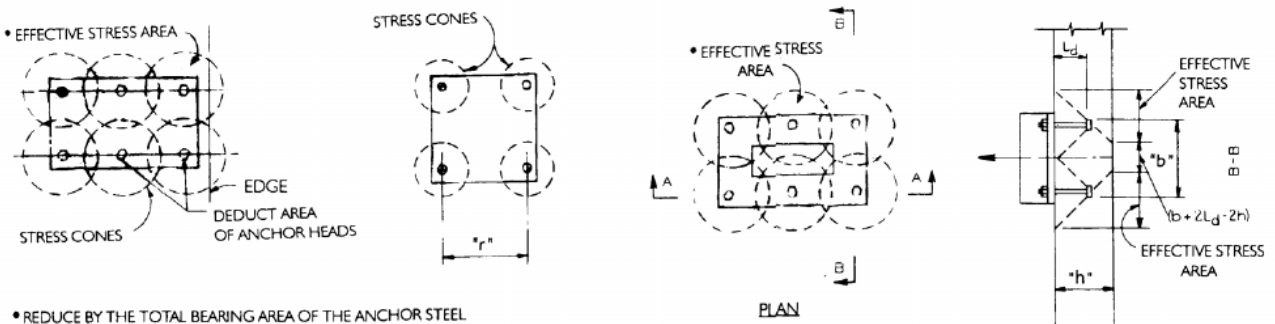


Figure 1.1 - ACI 349-85 (Projected Area of Failure Cone)

During the mid to late 1990's there was a methodology shift in determining the strength of anchored connections. This shift was driven by the demand for steel anchors to perform at a higher level and the need for a more flexible and reliable method of calculation. The Concrete Capacity Design (CCD) method (Fuchs, Eligehausen, & Breen 1995) was introduced as alternate means of determining the strength of concrete. The CCD method combines the visualization of the physical model represented by ACI 349-85, the accuracy of the κ -method and provides a more user-friendly breakout surface0 below (Fuchs, Eligehausen, & Breen 1995).

One of the largest improvements was the idealization of the projected failure surface as a prism formed at 35° (55° from the centerline of the anchor) as opposed to 45° (See Figure 1.3). The 35° angle is equivalent to the $1.5c_1$ that is used in multiple codes today. This use of a prism allows for a simpler calculation when determining the influence of free edges and overlapping anchors

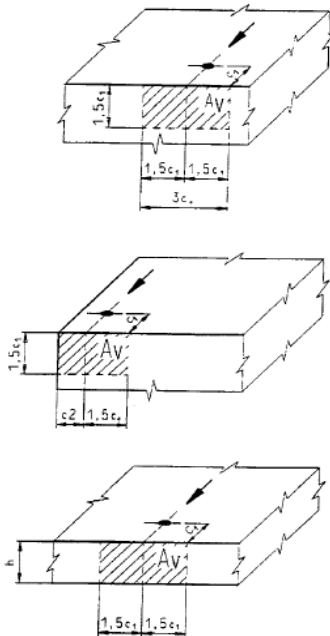


Figure 1.2 - Concrete Failure Surface with Reductions for Edges

(See Figure 1.2). With enough anchor specimens tested, it was found that the CCD method was consistent with average load at concrete failure.

Previously, brittle failure of concrete was avoided in designs due to the uncertainty in calculating the appropriate strength and the lack of test data to verify the average concrete

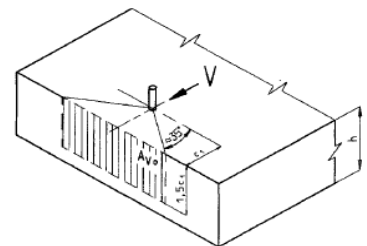
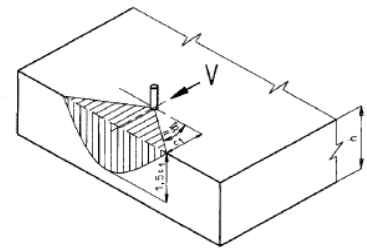


Figure 1.3 - Idealized Concrete Failure Surface

failure load. The CCD method proved to be a reliable method to determine concrete failure. These findings revolutionized the way the industry calculates and designs fastenings to concrete. Now that ductile or brittle design could be predicted with certainty, the applications for steel anchors increased significantly.

1.1.4 Current Method used to Determine Concrete Breakout in Shear

Currently, both ACI 318-14 and ACI 349-13 use the CCD approach as the governing method to determine concrete breakout strength. But, ACI Committee 349 only recently adopted the CCD method in the 2002 edition of the code, ACI 349-02. In ACI 349-85, the concrete breakout capacity calculates the projected concrete failure cone as the cylindrical section of uniform stress. Upon examination of European and U.S. standard calculation of capacity against the tested values, the CCD method agreed well with the average failure loads in the European tests (Fuchs et al. 1995). The study concluded that the average shear capacity over a range of spacing and embedment depths was accurately predicted by the CCD method; but also determined that the ACI 349-85 is overly conservative for anchors with small edge distances, while not conservative for larger edge distances (Fuchs et al. 1995). Notably, several equations provided by ACI 318-14 code are adaptations of equations from both the development of the CCD method as well as, the European code Comité Euro-International Béton, “Design of Fastenings in Concrete” (CEB). In 2006, another publication was completed titled, “Anchorage in Concrete Construction” (ACC) (Eligehausen, et al, 2006), that provides more explanation of the equations utilized in CEB.

The equations used to calculate the concrete capacity in ACI 318-14 and European codes all follow the same structure with similar modification factors to account for the influence of

edges, eccentric load, spacing, etc. See Table 1.1 – Table 1.5 for shear breakout capacity equations for ACI 318-14, ACI 349-85, CEB, CCD approach, and ACC text respectively.

Table 1.1 - Shear Breakout Equations used in ACI 318-14

Equation	Reference	Comment
$V_{cb} = \frac{A_{Vc}}{A_{Vco}} \psi_{ed,v} \psi_{c,v} \psi_{h,v} V_b$	(1)	Nominal Breakout Strength of Anchor
$V_b = \left(7 \left(\frac{l_e}{d_a} \right)^{0.2} \sqrt{d_a} \right) \lambda_a \sqrt{f'_c} (c_{a1})^{1.5} < 9 \lambda_a \sqrt{f'_c} (c_{a1})^{1.5}$	(2)	Basic Concrete Breakout Strength limited by large diameter anchors
$\psi_{ed,v} = 0.7 + 0.3 * \left(\frac{c_2}{1.5c_1} \right) \leq 1$	(3)	Modification Factor for Influencing edges
For anchors where analysis indicates no cracking $\psi_{c,v} = 1.4$ For anchors where analysis indicates cracking: $\psi_{c,v} = 1.0$ for cracked concrete without supplementary reinforcement or reinforcement smaller than No. 4 bar $\psi_{c,v} = 1.2$ for cracked concrete with reinforcement of a No. 4 bar or greater between the anchor and the edge $\psi_{c,v} = 1.4$ for cracked concrete with reinforcement of a No. 4 or greater between the anchor and the edge, and the reinforcement enclosed within stirrups spaced not more than 4in.	(4)	Modification Factor for Uncracked and Cracked Concrete with and without supplemental reinforcement
$\psi_{h,v} = \sqrt{\frac{1.5c_{a1}}{h_a}} \geq 1$, when $h_a > 1.5c_{a1}$	(5)	Modification Factor for Member Size

Table 1.2. Shear Breakout Equations used in ACI 349-85

Equation	Reference	Comment
$V_c = 4\phi\sqrt{f'_c}$	(6)	Strength of Concrete under uniform stress

Table 1.3. Shear Breakout Equations used in CEB – “Design of Fastenings”

Equation	Reference	Comment
$V_{Rk,c} = V_{Rk,c} * \psi_{A,v} * \psi_{h,v} * \psi_{s,v} * \psi_{\alpha,v} * \psi_{ucr,v} [N]$	(7)	Characteristic resistance of anchor
$\psi_{A,v} = A_{c,v}/A_{c,v}^0$	(8)	Factor to account geometric effects
$V_{Rk,c}^0 = k_4 * d_{nom}^{0.5} * \left(\frac{l_f}{d_{nom}} \right)^{0.2} * f_{ck}^{0.5} * c_1^{1.5} [N]$ $k_4 = 0.5 [N^{0.5} / mm]$	(9)	Characteristic resistance of anchor without influence
$\psi_{h,v} = \left(\frac{1.5c_1}{h} \right)^{1/3} \geq 1$, when $h_a > 1.5c_{a1}$	(10)	Factor to account for member thickness
$\psi_{s,v} = 0.7 + 0.3 * \left(\frac{c_2}{1.5c_1} \right) \leq 1$	(11)	Factor to account for edge influence

$\psi_{\alpha,v} = 1.0$ for $\alpha < 55^\circ$	(12)	Factor to account of angle of applied shear load
$\psi_{ucr,v} = 1.0$ for cracked concrete without edge reinforcement $\psi_{ucr,v} = 1.2$ for cracked concrete with straight edge reinforcement $\psi_{ucr,v} = 1.4$ for cracked concrete with edge reinforcement and closely spaced stirrups	(13)	Factor to account for uncracked concrete or cracked concrete with and without reinforcement

Table 1.4. Shear Breakout Equations proposed for CCD Approach

Equation	Reference	Comment
$V_n = \frac{A_v}{A_{vo}} * \psi_4 * \psi_5 * V_{no}$	(14)	Nominal Concrete Breakout Strength
$\psi_5 = 0.7 + 0.3 * \left(\frac{c_2}{1.5c_1} \right)$	(15)	Tuning Factor for stress distribution at corner
$V_{no} = 13 \left(\frac{1}{d_o} \right)^{0.2} \sqrt{d_o} * \sqrt{f'_c} * c_1^{1.5}$ [lb] (a) $V_{no} = \left(\frac{1}{d_o} \right)^{0.2} \sqrt{d_o} * \sqrt{f'_c} * c_1^{1.5}$ [N] (b) $l \leq 8d_o$ [mm]	(16)	Basic Concrete Breakout Strength Activated bearing length of fastener

Table 1.5. Shear Breakout Equations used in “Anchorage in Concrete Construction”

Equation	Reference	Comment
$V_{Rk,c} = V_{Rk,c} * \psi_{A,v} * \psi_{h,v} * \psi_{s,v} * \psi_{\alpha,v} * \psi_{ucr,v}$ [N]	(17)	Characteristic resistance of anchor
$V_{Rk,c}^0 = 0.45 \sqrt{d_{nom}} * \left(\frac{l_f}{d_{nom}} \right)^{0.2} * \sqrt{f_{ck,cube}} * c_1^{1.5}$ [N]	(18)	Characteristic resistance of anchor without influence
$\psi_{h,v} = \sqrt{\frac{1.5c_1}{h}} \geq 1$, when $h_a > 1.5c_1$	(19)	Factor to account for member thickness
$\psi_{s,v} = 0.7 + 0.3 * \left(\frac{c_2}{1.5c_1} \right) \leq 1$	(20)	Factor to account for edge influence
$\psi_{\alpha,v} = 1.0$ for $\alpha < 55^\circ$	(21)	Factor to account of angle of applied shear load
$\psi_{ucr,v} = 1.0$ for cracked concrete without edge reinforcement $\psi_{ucr,v} = 1.2$ for cracked concrete with straight edge reinforcement $\psi_{ucr,v} = 1.4$ for cracked concrete with edge reinforcement and closely spaced stirrups	(22)	Factor to account for uncracked concrete or cracked concrete with and without reinforcement

Although ACI 349-85 criteria places a strict limitation on the position of the anchor, it does provide a conservative lower bound prediction for anchors with small edge distances. This limitation is evident when examining how simplistic the equation is for concrete strength. This generally is not applicable and will not govern the design.

ACI 318-14, CEB, and ACC are all derived from the research in CCD approach proposed in 1995. Upon examination of the nominal or characteristic basic breakout strength (Table 1.1 Eq. (2), Table 1.3 Eq. (9) and Table 1.5 Eq. (18), respectively), there is considerable difference between the codified equations and the CCD approach. ACI 318-14 basic concrete breakout strength includes the constant 7, instead of 13. European code, CEB utilizes the factor $k_4 = 0.5$, instead of the constant 1.0, originally proposed. ACI 318-14 commentary states, “*the constant, 7, in the shear strength equations was determined from test data reported...at the 5 percent fractile adjusted for cracking*” (ACI 318-14). CEB does not provide a justification for the reduction resulting from $k_4 = 0.5$. In 2006, characteristic breakout strength used in CEB, was adjusted to account for 5% fractile and cracked concrete similar to ACI (Eligehausen, et al, 2006b). The modification factors for concrete, $\Psi_{c,v}$ and $\Psi_{ucr,v}$, were determined through experimental values of failure of anchors in cracked concrete. It was found that anchors in cracked concrete failed at loads between 70% and 75% of uncracked concrete (Eligehausen and Balough, 1995). To validate the factor, $\Psi = 1.4$, which increases the shear breakout strength the following calculation is given as $1/1.4 = 0.714 \rightarrow 71.4\%$ of uncracked failure strength. The adjustment the nominal or characteristic breakout strength for 5% fractile and cracking is given below:

For ACI 318-14:

$$(\text{Assume } 5\% \text{ fractile} = 0.753) V_{b(\text{adj})} = V_{b(\text{avg})} \times (5\% \text{ frac.} \times 1 / \Psi_{c,v}) = V_b \times (0.753 \times 1/1.4)$$

$$V_{b(\text{adj})} = V_{b(\text{avg})} \times 0.538$$

- proposed constant of 13, the adjusted equation for nominal breakout strength, V_b is equal to:

$$V_{b(\text{adj})} = 13 \times 0.538 = 7 (V_{b(\text{avg})})$$

For CEB/ACC: (Specified 5% fractile = 0.7) $V_{Rk,c(\text{adj})} = V_{Rk,c(\text{avg})} \times (5\% \text{ frac.} \times 1 / \Psi_{c,v}) = V_b \times (0.7 \times 1/1.4)$

$$V_{Rk,c(adj)} = V_{Rk,c(avg)} \times 0.50$$

- constant of 1.0 for CEB, the adjusted characteristic breakout strength, $V'_{Rk,c}$ is equal to:

$$V_{Rk,c(adj)} = 1.0 \times 0.50 (V_{Rk,c(avg)})$$

- constant of 0.9 for ACC, the adjusted characteristic breakout strength $V'_{Rk,c}$ is equal to:

$$V'_{Rk,c} = 0.90 \times 0.50 = 0.45$$

Reducing CCD approach for shear breakout was necessary because the equation predicts the mean value at which the concrete would fail. This was a purely empirical approach and did not include any statistical analysis. Similar to the revised equation given in ACC compared to CEB code, the modification factor for member thickness (Eq. (10) and Eq. (20), respectively) were also changed to be consistent with testing.

1.1.5 Size Effect of Anchor Bolts

In the case of tensile loading, the required embedment depth is a very important factor when choosing an anchor for application. Through testing and numerical studies, it has been determined that the ultimate concrete breakout strength is not directly proportional to the embedment depth of the anchor. This concept is called “Size effect”. Size effect can be defined as: *“the fracture front blunted by a zone of micro-cracking causing deviations from the structural size effect known from linear elastic fracture mechanics.”* (Bazant 1984). Based on the theory proposed by Bazant, studies have been conducted to determine the amount of influence and at what range of embedment depths does size effect apply to. In 1991, Eligehausen and Ozbolt proposed a formulation based on numerical finite element modeling that included the size effect was given as:

$$F_n = a_1 \sqrt{E G_f} d^{3/2} \quad (23)$$

This formula was later refined via testing to the following:

$$F_u = 2.2 f_{cc}^{0.5} h^2 \left(1 + \frac{h}{100}\right)^{-0.5} \quad (24)$$

The terms h and d are the embedment depths, respectively. Simplification of $F_n = a_1 \sqrt{EG_f} d^{3/2}$ (23), would result in the embedment depth raised to the power of 3/2, which is consistent with the numerical analysis previously completed. This equation predicts a gradual transition from a plastic solution (no size effect) for small embedment depths to a linear fracture mechanics solution (largest size effect) for large embedment depths (Eligehausen et al. 1992).

The transition between the plastic and fracture mechanics solution can be seen in Figure 1.4. This conclusion falls directly within the description of size effect theory (Bazant 1984). As embedment depth increases to a point the transfer effects less of the surrounding concrete is consistent with other mechanics of material principles.

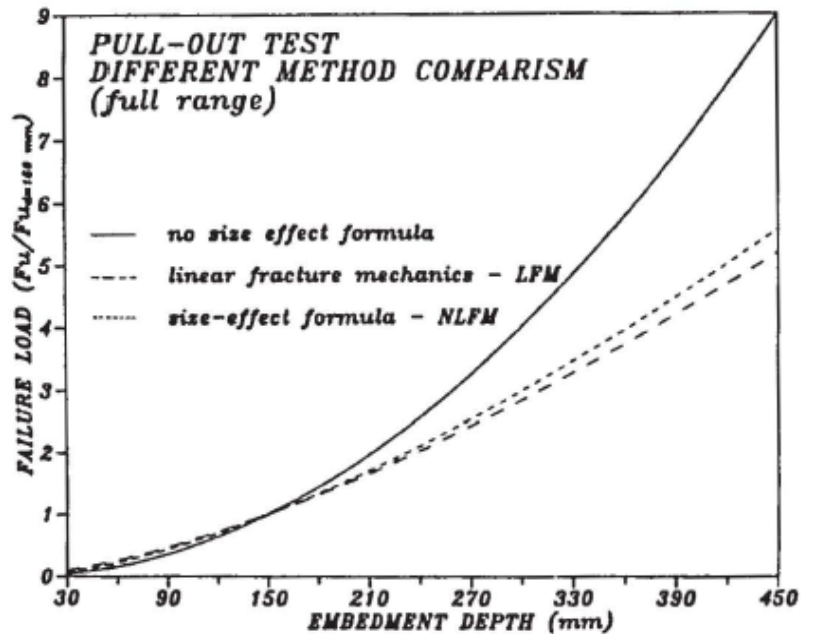


Figure 1.4 - Embedment Depth and Failure Load Curve

Since the concept of size effect is based on a localized zone of microcracking, the principles of fracture mechanics for a portion of concrete loaded in tension are applied to concrete loaded in shear. Both ACI 318-14 and CEB “Design of Fastenings” consider size effect in the calculation of concrete breakout in shear by incorporating the edge distance parameter raised to the 3/2 power (i.e. $ca_1^{1.5}$).

1.1.6 Current Standard Definition of Supplemental Reinforcement

Cast-in steel anchors that are used in any type of reinforced concrete structure will have some type of reinforcement near the embedment. Simply assuming that any reinforcement placed within the failure surface will supplement the

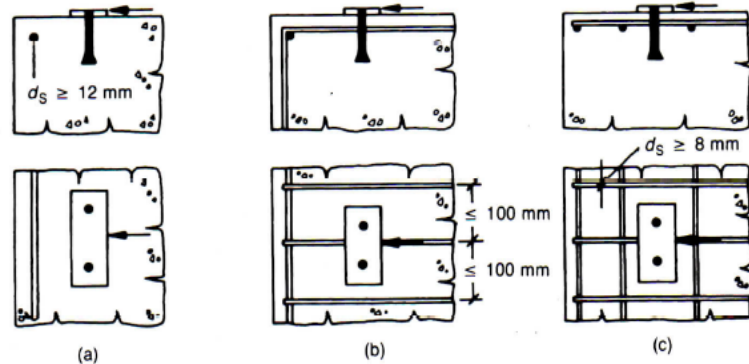


Figure 1.5 - Lateral Distribution of Longitudinal and Edge Reinforcement – CEB

concrete strength is incorrect. Studies have shown that there are limitations on how much of the existing steel can be considered, as well as the increase for nominal shear breakout capacity. ACI 318-14, CEB, and ACC specify several conditions for a modification factor used to increase the shear capacity based on whether or not the concrete is cracked in addition to the presence of reinforcement (See Table 1.1, Table 1.3 and Table 1.5 for commentary). When reinforcement is present, but not specially designed for the application, the concrete breakout strength is multiplied by a modification factor. The largest modification factors are applied to uncracked concrete during service loading ($\Psi_{c,v} = 1.4$) and cracked concrete with closely spaced stirrups and edge reinforcement ($\Psi_{c,v} = 1.4$). The closely spaced stirrups were originally required to provide sufficient confinement to meet seismic design criteria. This would prevent spalling of the corner and weakening of the structure. Edge reinforcement and stirrups spacing are based on the testing presented in ACC text. ACI 318-14 and CEB specify a minimum bar size of No. 4 (1/2") and 12 mm, respectively. Edge reinforcement must be confined with the stirrups spaced no farther than 4 in ACI 318-14 and 100 mm for CEB (See Figure 1.5). The distance or quantity of stirrups is not mentioned in the description. Using a failure surface of $3.0c_{a1}$ it would seem that

the reinforcement only needs to be installed within that distance, but this information is missing from code. Clarification would be beneficial for a minimum diameter on the stirrups as well. Not specifying the size of the stirrups leaves the decision to the judgement of the designer. These descriptions are open-ended and leave room for interpretation. Without a more detailed description, the designer would be forced to err towards a potentially over conservative design.

If the applied loading still exceeds the shear capacity with all the appropriate modification factors, supplemental reinforcement is permitted to be incorporated to increase the load-bearing capacity of the fastening. The location, size and anchorage, or development length, of the rebar all have a range in which the reinforcement is considered effective. Typically, two methods of supplemental reinforcement are used; stirrups with edge reinforcement or hairpins that enclose the fastener.

When dealing with supplemental stirrups and edge reinforcement, the position of steel is an important aspect to examine. Intuitively, we understand that the closer a support is to an applied load, the more load that support will resist. It is often said, stiffness attracts load. Supplemental reinforcement follows that same concept. Decreasing the distance between the stirrups and anchor, increases the effectiveness. Research has been conducted to analyze how the effectiveness of reinforcement changes with position relative to the fastening. Test shows that

stirrups combined with edge reinforcement will increase the load-bearing capacity, this can be seen in the difference between curve 1 and 2 in Figure 1.6. Even though, the projected concrete

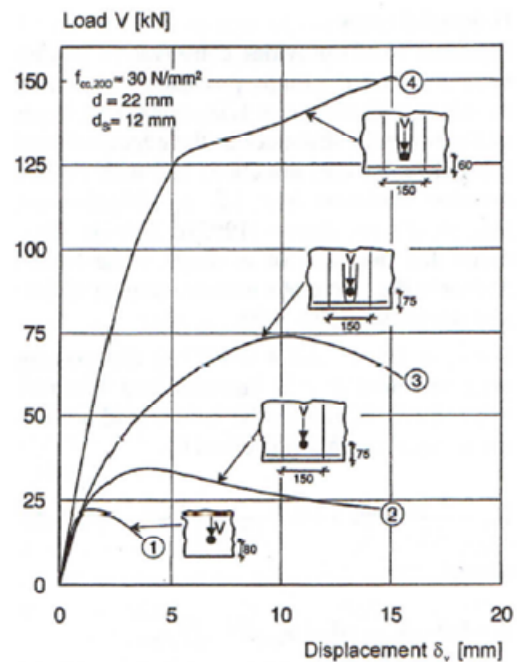


Figure 1.6 - The effect of reinforcement on load-bearing behavior of single anchors close to an edge – (Eligehausen 2006b)

failure area has a width of $3.0h_{ef}$, only the reinforcement near the anchor is considered effective from a calculation stand-point. Bars placed within the lesser of $0.3c_{a2}$ and $0.5c_{a1}$ from the centerline of the anchor are considered effective in increasing the strength of concrete according to ACI 318-14 (See Figure 1.7).

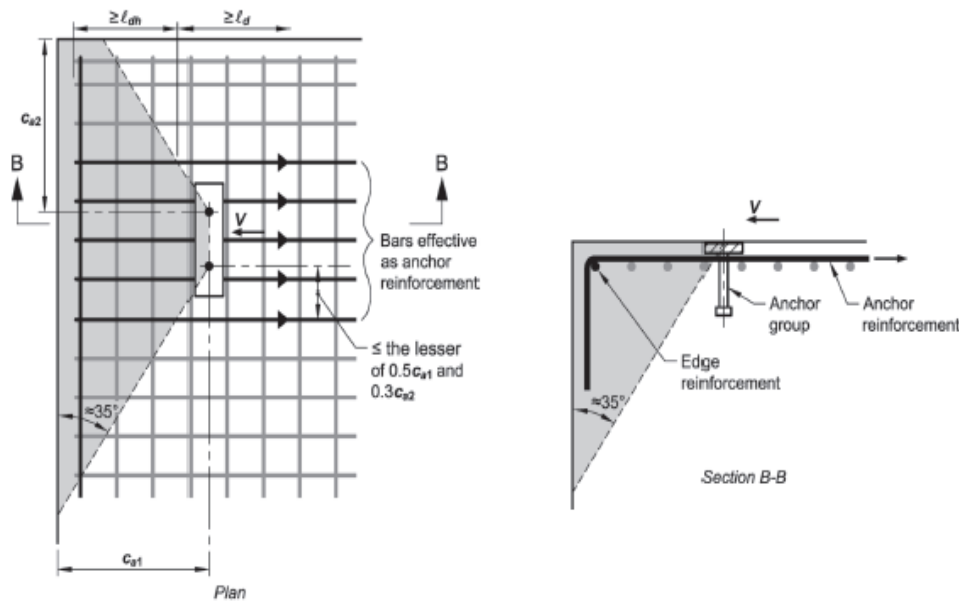


Figure 1.7 - Lateral Distribution of Longitudinal and Edge Reinforcement - ACI 318-14

The depth at which the reinforcement is placed has a very drastic impact on how the fastening will perform. Hairpins and stirrups are typical reinforcement details used to confine the concrete around a steel anchor. The proximity of the rebar relative to the shaft of the anchor, as well as the distance from the surface of concrete, have been tested.

A series of specimens (56 total) with varying perpendicular edge distances and reinforcement details were tested to investigate the effectiveness of hairpins placed around anchors and provide guidelines as design criteria (Klinger et al 1982). The study was comprised of hairpins that were placed within varying offsets from the shaft of the anchor, as well as with varying depths from the surface of concrete (See Figure 1.8). Plain concrete with anchors and large (non-critical) edge distances were used as a control group for comparison. The results of

the testing showed that with the addition of the hairpin, the anchors with short edge distances were able to reach loads as high as the anchors with large edge distances in plain concrete.

Many of the tests did not reach the full shear capacity of the steel anchor due to excessive deflection as a result of concrete spalling in front of the anchor. Of the four types of hairpin reinforcement studied, the spalling loads were highest in the “Type 1” hairpin detail (See Figure 1.8), which were approximately 40% higher than “Types 2-4”.

The spalling load increase was attributed to the biaxial compression of the concrete in front of the anchor in “Type 1”, as opposed to the stress concentrations in the concrete around the reinforcement seen in “Types 2-4”. The authors also conclude that placing the hairpin reinforcement as close as possible to the anchor provided good performance at the ultimate load. When the distance of the reinforcement to the surface of concrete (cover) is increased, the load-displacement also increased (i.e.

decreased effectiveness). Another experiment conducted in 2013 agreed with the results from testing from Klinger (Petersen, Zhao 2013).

This increased performance was validated by the concept of anchor stiffness influence on load-bearing capacity. Behavior of anchors with applied tension in cracked concrete, analyzed to examine the influence of crack size. Cast-in-place and post-installed anchors were tested in cracked concrete with varying crack widths and the load-displacements were noted during the

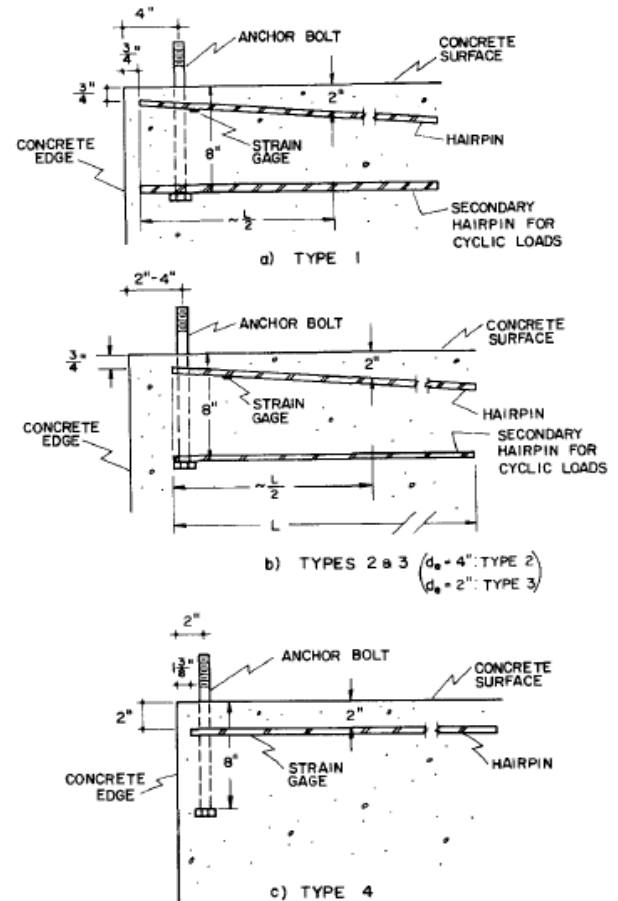


Figure 1.8 - Hairpin Reinforcement Details tested

experiment (Eligehausen et al 1995). A reduction of 25% concrete cone failure load was noted due to anchor in or near cracks when compared to uncracked concrete. This shows that the anchor stiffness directly impacts the load carrying capacity of the concrete failure cone.

Providing reinforcement close to the surface which restrains the anchor and confines the concrete is the most effective way to increase the stiffness of the anchor itself. Similar results were found in another study with large diameter anchors with deep embedment. It was determined that the hairpin reinforcement increased the concrete breakout capacity, but was still less than the anticipated ultimate load for the steel based on yield stress (Lee et al. 2010).

The resulting data of the previous studies provided the basis for the requirement specified in both ACI 318-14 and CEB “Design of Fastenings”. The American Society of Civil Engineers (ASCE), published a document specifying guidelines for design stirrup reinforcement for concrete pedestals (Widianto; Owen, J.; and Patel, C, 2010). The design example using Strut-and-Tie method for determining the corresponding tensile loads in either stirrup located 2 in and 5 in below the surface. ACI 318-08 comments on pedestal reinforcement, “*Confinement improves load transfer from the anchor bolts to the column or pier for situations where the concrete cracks in the vicinity of the bolts*”

(ACI 318-08). The cracking in the vicinity of the anchors bolts is likely referring to the radial stress that propagates outwards from the anchor when axial load is applied. This ASCE design method makes use of the reinforcement by modeling the

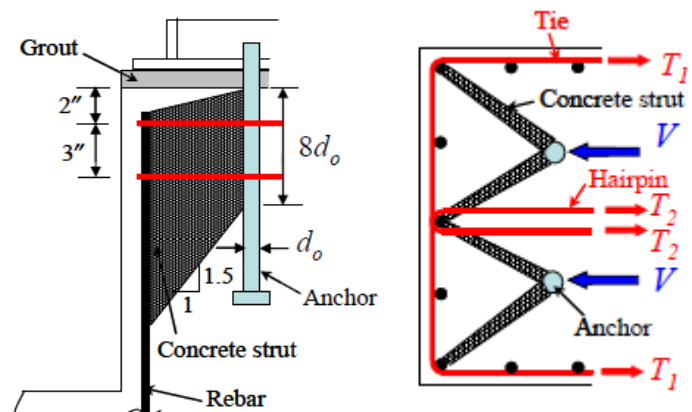


Figure 1.9 - ASCE Stirrup Reinforcement Detail using STM

shear load as a distributed load along the activated portion of the anchor ($8d_o$, which is consistent

with previous studies and codes) and is shared between both layers of reinforcement (See Figure 1.9). This type of analysis does not directly follow the parameters set forth by ACI 318-14 or CEB, but STM analysis is permitted in ACI 318-14 per commentary R17.5.2.9 (See Figure 1.9).

If all of the preceding criteria are met, but the reinforcement is not properly anchored (or developed), the design will not be effective and will not adequately withstand the load. Peak loads less than the ultimate load of the reinforcement were attributed to spalling of concrete and insufficient anchorage. The total shear that can be resisted is determined by the summation of the number of stirrups developed within the failure surface or number of bar developed outside the failure surface for hairpin reinforcement (See Table 1.6).

Table 1.6 - Development Length and Hanger Reinforcement Capacity

Reference	Equation	Reference	Comment
ACI 318-14	$l_d = \left[\frac{f_y \psi_t \psi_e}{25 \lambda \sqrt{f'_c}} \right] d_b \geq 12 \text{ [in]}$	(25)	Development length for bars with confining reinforcement
	Or $l_d = \left[\frac{3 f_y \psi_t \psi_e}{50 \lambda \sqrt{f'_c}} \right] d_b \geq 12 \text{ [in]}$	(26)	Development length for bars without confining reinforcement
	Or $l_d = \frac{3}{40} \left(\frac{f_y}{\lambda \sqrt{f'_c}} \right) \left[\frac{\psi_t \psi_e \psi_s}{\left(\frac{c_b + K_{tr}}{d_b} \right)} \right] d_b \geq 12 \text{ [in]}$	(27)	Refined Development length for bars with confining reinforcement
CEB, “Design of Fastenings”	$N_{Rd,a} = \Sigma(l_1 * u * 2 * f_{bd}) \text{ [N]}$	(28)	Anchorage failure of the hanger reinforcement in the concrete

ACI 318-14 development lengths have multiple ways to calculate the minimum distance required for different applications. CEB equation is more focused on calculating the design resistance with a given development length. ACI 318-14, CEB, and ACC agree that when stirrup reinforcement is used, the bars must be anchored on either side of the failure surface because the bars are assumed to yield (See Figure 1.11, 1.12, 1.10 respectively). If hairpin reinforcement is utilized the bars only need to be development outside of the failure surface (See Figure 1.11 and 1.12). Since the bar is placed in very close proximity to the shaft of the anchor, the load is directly transferred to the reinforcement.

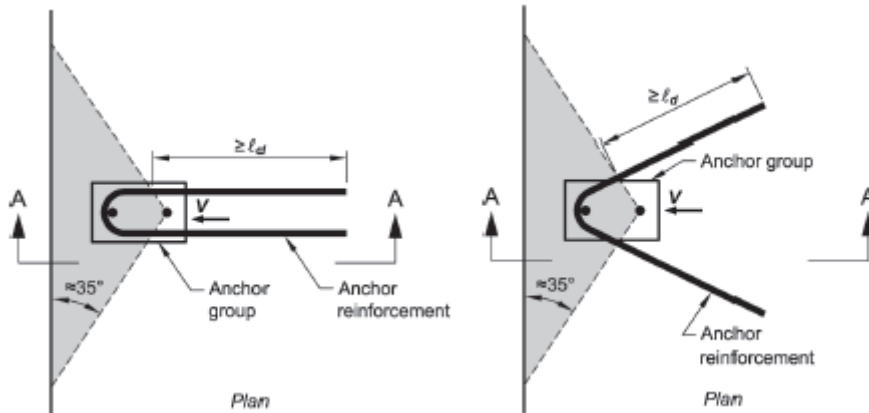


Figure 1.10 - Development Length of Suppl. Reinf. using Hairpins ACI 318-14

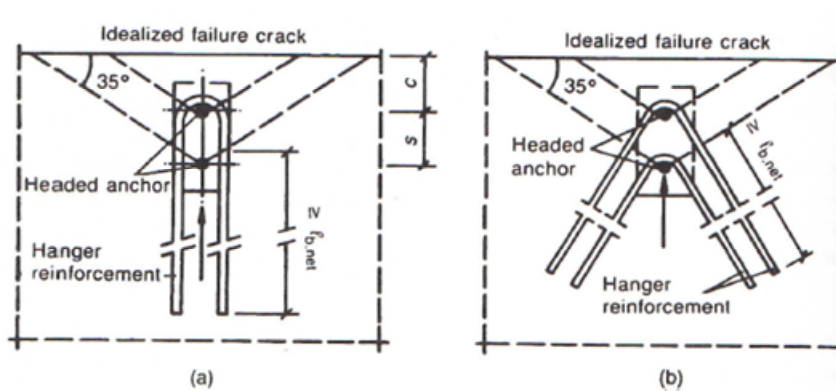


Figure 1.11 - Development Length for Hairpin Reinforcement beyond failure surface - CEB

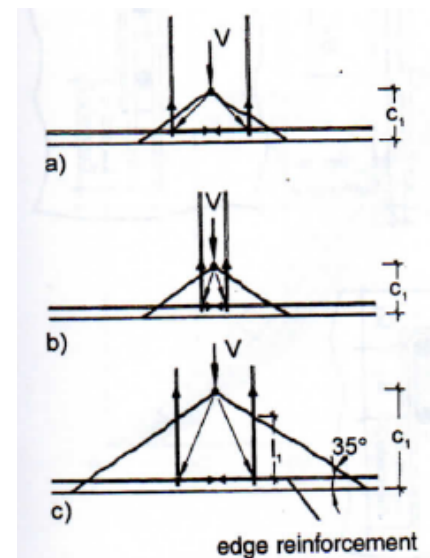


Figure 1.12 - Stirrup Reinforcement Development Length - ACC

1.1.7 Sizing and Capacity of Shear Reinforcement

Safety factors or strength reduction factors are a critical part of any anchorage design and can vary greatly based on the application or failure mode. CEB uses a partial safety factor of $\gamma_{ms,1} = 1.15$ to reduce the allowable load for both the steel fastener and the concrete failure. Between the two codes, only ACI 318-14 separates the failure modes for brittle concrete failure with and without reinforcement present. “Condition A” considers the effect of reinforcement being present. ACI R17.3.3 specifies that there does not need to be an explicit design for the reinforcement if it is not sized to resist the full shear load. The capacity increased is minimal (i.e. $\phi = 0.75$ for Condition A and $\phi = 0.70$ for Condition B). Strength reduction for supplemental reinforcement is equal to $\phi = 0.75$.

The original testing conducted to determine the influence of reinforcement concluded that only deformed bars of 16 mm (~ No. 5 U.S. standard size) are allowed. As reinforcing bars begin to increase in size beyond 16 mm, they may not be able to develop yield stress. If bars do not reach yield strength, then there is load sharing between the concrete and steel bars which is not permitted based on the completed research. Flexibility of the reinforcement is cited as the probable reason that larger bars are less effective than smaller diameters (<16 mm or No. 6 max). *“...supplementary reinforcement did increase capacity. The increase, however, was much less than what would have been achieved for complete load transfer to the stirrups on either side of the anchorage...This is likely due to the flexibility of the hairpins and to the large displacements of the anchor required to develop complete yield of the hairpins,”* (Lee et al. 2010). The limitation of reinforcing bars to 16 mm or No. 5 is to ensure yielding of the reinforcing prior to excessive load transfer into the concrete. Current practice is to size the reinforcement to resist the applied shear load and neglect any contribution from the concrete itself. Neither ACI 318-14 nor

CEB specify how the load is distributed to the reinforcement when there are multiple bars on either side of the failure surface. ACC authors write, “*The shear capacity of the anchorage is derived by summing the capacities for all stirrup legs...whereby only those stirrups legs near the surface should be included*” (Eligehausen, et al, 2006b). Since the deformation in the concrete failure prism is relatively small, any reinforcement placed within the permitted range will share the load equally.

Table 1.7 - Shear Strength of Supplemental Reinforcement

Reference	Equation	Reference	Comment
ACI 318-14	$V_{sr} = A_s \times f_y$	(29)	Nominal Strength of Supplemental reinforcement
	$V_u = \phi V_{sr} = \phi A_s \times f_y$ [lb]	(30)	Ultimate Strength of Reinforcement
CEB, “Design of Fastenings”	$V_{Rk,s1} = k_7 \times \eta_2 \times A_s \times f_{yk}$ [N] k_7 = efficiency factor = 0.5 η_2 = # of bars in hanger reinf. per anchor	(31)	Steel Failure of hanger reinforcement (applies to stirrups and hairpins)
	$V_{Rd,s1} = V_{Rk,s1} / \gamma_{Ms1}$ [N]	(32)	Factored Steel Failure
Anchorage in Concrete Construction	$V_{u,s} = 2 \times \eta_1 \times A_s \times f_y$ [N] η_1 = efficiency factor varies = 0.5 to 1.0 $\eta_1 = 1.0$ for reinf. against anchor $\eta_1 = 0.5$ for reinf. with gap between anchor	(33)	Load Carried by single bar of hairpin hanger reinforcement with efficiency factor, η
	$V_{Rd,s1} = V_{Rk,s1} / \gamma_{Ms1}$ [N]	(34)	Factored Steel Failure for hairpins
	$V_{u,a} = \pi \times d_s \times l_1 \times f_{bm} / \alpha_a \leq A_s \times f_y$ [N] f_{bm} = bond strength [N/mm ²] $\alpha_a = 0.7$	(35)	Load carried by single bar with given development length for stirrups
			Factor to take into account hook or welded transverse bars
	$V_{Rd,s1} = V_{u,a} / \gamma_{Ms1}$ [N]	(36)	Factored Steel Failure for stirrups

The most notable difference between the equations for supplemental or hanger reinforcement are the factors of safety and efficiency applied to the nominal strength of steel. ACI 318-14 only applies a strength reduction factor, of 0.75, which includes the decreased efficiency for placement below the applied shear. ACC provides two equations used to calculate load carried by either stirrups or hairpins. Equation 33 is consistent with Equation 31 in terms of efficiency factors and the number of bars included ($k_7 = 0.5$ and $\eta_1 = 0.5$ to 1.0).

European code, CEB, apply a factor of safety $\gamma_{Ms1} = 1.15$, which equates to a reduction of $1/1.15 = 0.869$. This is in combination with the efficiency factor, $k_7 = 0.5$ and $\eta_1 = 0.5(\text{min})$. The total strength reduction is approximately equal to 0.43 for both hairpins and CEB stirrups. ACC does not specify any reduction for efficiency in Equation 35. According to ACC equation for stirrup capacity is only reduced by the factor of safety, $\gamma_{Ms1} = 1.15$ which is less conservative compared to the ACI 318-14 reduction.

1.2 Problem Statement

Based on the discussions above, the code might be too conservative and can be expanded. Therefore, this study will examine this by using FEA to determine the load-bearing capacity when reinforcement is spaced at a distance greater than 4 in. This would help in alleviating design costs, supply expenses, labor and time – thus improving the concrete construction industry.

CHAPTER 2: FINITE ELEMENT ANALYSIS

2.1 Introduction

Finite Element Analysis programs are powerful tools that are often used to analyze complex problems that arise in the engineering field. Accurately modeling reinforced concrete structures has always been a difficult task to achieve. The FE program, ABAQUS, is capable of analyzing the nonlinear properties of concrete. In this model, the stresses within the concrete and reinforcement are generated by applying a load to the steel anchor, similar to a typical connection designed for a structure. Shear loading is applied via a specified displacement equal to 1 inch towards the perpendicular edge. Using a displacement-controlled method will result in a peak reaction forces which can then be compared to values calculated using approved code equations. In this model, the failure mechanisms will include concrete crushing and cracking. These failure mechanisms can be accounted for by specifying material damage properties. ABAQUS provides a method to calculate compression and tension damage values based on previous research. Tension damage is caused by cracks begin to open and redistribute stress into the surrounding areas and creating inelastic strain. Concrete compression damage is caused by concrete strain exceeding 0.003 in. In both cases the damage parameter is calculated by the following expression:

$$d = 1 - \frac{\sigma}{\sigma_{\text{peak}}} \quad (37)$$

Establishing an unreinforced or “plain” model control used as the control group for the subsequent tests is critical. This is done to validate that the concrete properties used are consistent with the expected failure load. Using the validated “control” model the reinforced models can be made. The calibration model will be designed in accordance with ACI 318-14. This will include edge reinforcement between the anchor and free edge of concrete as well as,

steel stirrups spaced at 4 inches along the edge. The calibration model can also be compared to code values for reinforced concrete. Once these models are validated the experimental models with varying stirrup spacing are analyzed. FE models will be able to predict the peak failure load of the different reinforcement configurations.

2.2 Model Design

2.2.1 Model Geometry

Four models are used throughout this study; (1) a simple concrete model without reinforcement (important in validating the material properties from code), (2) a concrete model with the recommended 4in reinforcement spacing, (3) an experimental concrete model with 6 in reinforcement spacing, and (4) another experimental concrete model with 8in reinforcement spacing. All models maintain the same geometry throughout the study, and appear as follows;

The steel anchor used in all of the models is created as a deformable solid revolution with the following geometry:

Length: 6-1/2"
Anchor Head: Ø1-5/8" x 1/2"
Shaft: Ø3/4" x 6"

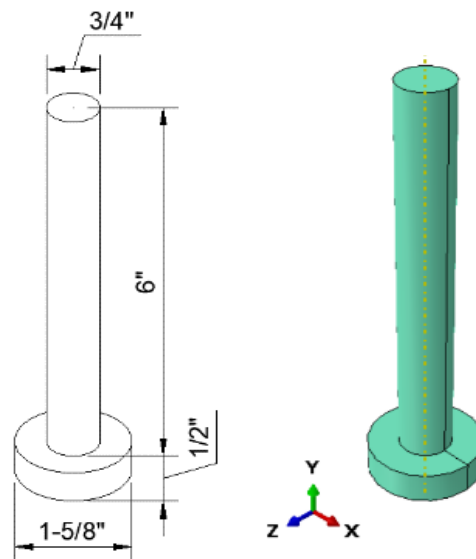


Figure 2.1 - Dimensions of Steel Anchor; All Model

The concrete block geometry was determined such that the projected failure surface would not be reduced by any adjacent edges (See Appendix for calculations regarding concrete block dimensions). An edge distance of 12 in was chosen to provide adequate distance away from the edge to allow for stress and tensile damage to spread to the adjacent steel reinforcement for the experimental models. Size effect of this model does not need to be considered any more than what is already assumed in the equations used to determine the anticipated failure loads. According to ACI 318-14, anchors with embedment of 11 in to 25 in exhibit failure loads that are consistently underestimated when using $h_{ef}^{1.5}$. An alternate equation is used to calculate a less conservative prediction for nominal concrete breakout failure when embedment exceeds 11 in. Applying this same concept and mechanics to a shear loading application, as well as rounding to a convenient distance of 12 in, the edge distance is justified for this study. With the perpendicular edge distance set equal to 12 in, the total length must be greater than $3.0c_{a1}$. The member depth is also sized such that it will not influence the failure surface; therefore, the member depth must be greater than $1.5c_{a1}$ (See Appendix for hand calculations). This results in a concrete domain with the following dimensions:

Length: 24"
Depth: 24"
Width: 40"

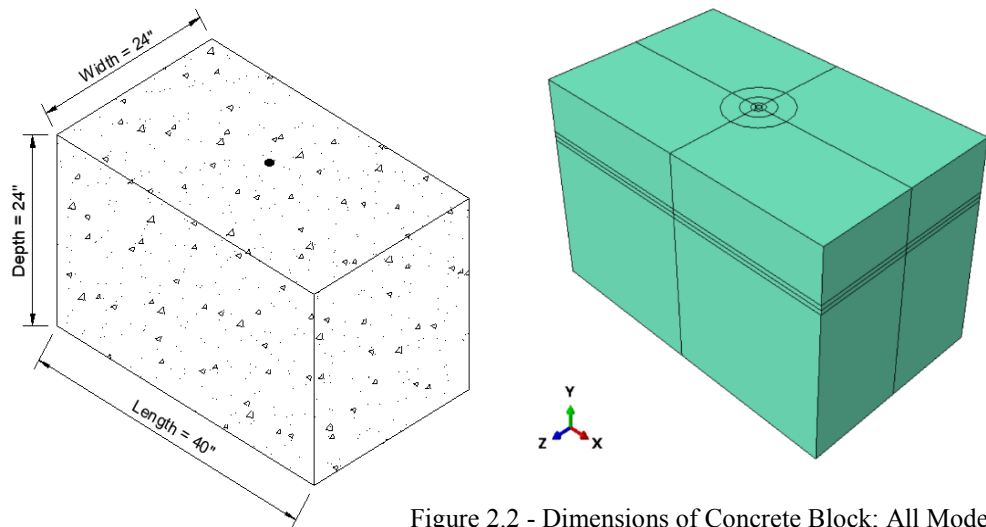


Figure 2.2 - Dimensions of Concrete Block: All Models

Stirrups are detailed in accordance with ACI 318-14 to include concrete cover of 1 inch and minimum bend radius for No. 5 deformed bars equal to $6d_a$ or $3\text{'-}3/4\text{'}$. Embedment constraint was used to model the interface between the internal surface of concrete and the external surface of the reinforcement.

Bar: No. 5 bar ($\text{Ø}5/8\text{'}$)
Length = Width: 22' or $1\text{'-}10\text{'}$ overall

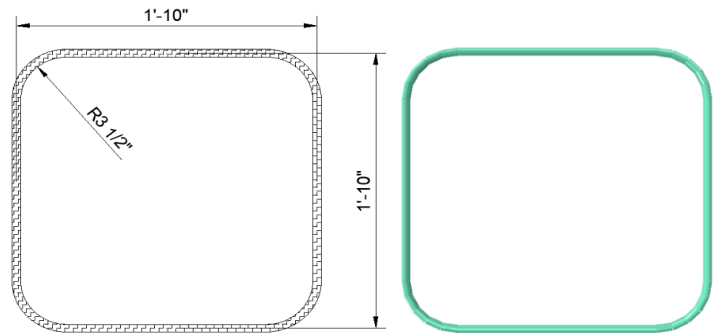


Figure 2.3 - Dimensions of Stirrup Design used Throughout Study

Edge reinforcement is detailed according to ACI 318-14 deformed bar. Embedment constraint was used to model the interface between the internal surface of concrete and the external surface of the reinforcement.

Length: 40'
Bar: No. 4 ($\text{Ø}1/2\text{'}$)

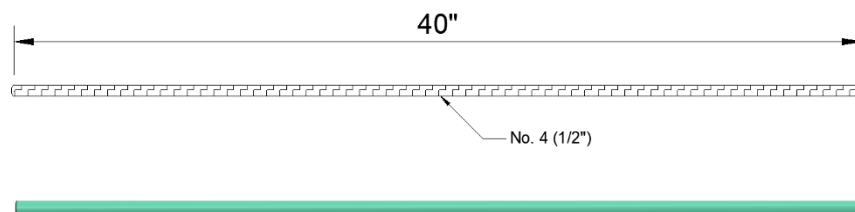


Figure 2.4 - Edge Reinforcement Dimensions used Throughout Study

Each model has identical boundary conditions and specified loading. Using a fixed boundary condition along the bottom surface ensures that the tensile or compressive stresses in the concrete are unaffected by any external reactions. As previously mentioned, a displacement-controlled boundary condition is applied to the top surface of the embedded anchor. The benefit to use displacement is that the peak load value is easily found for a given force vs displacement curve.

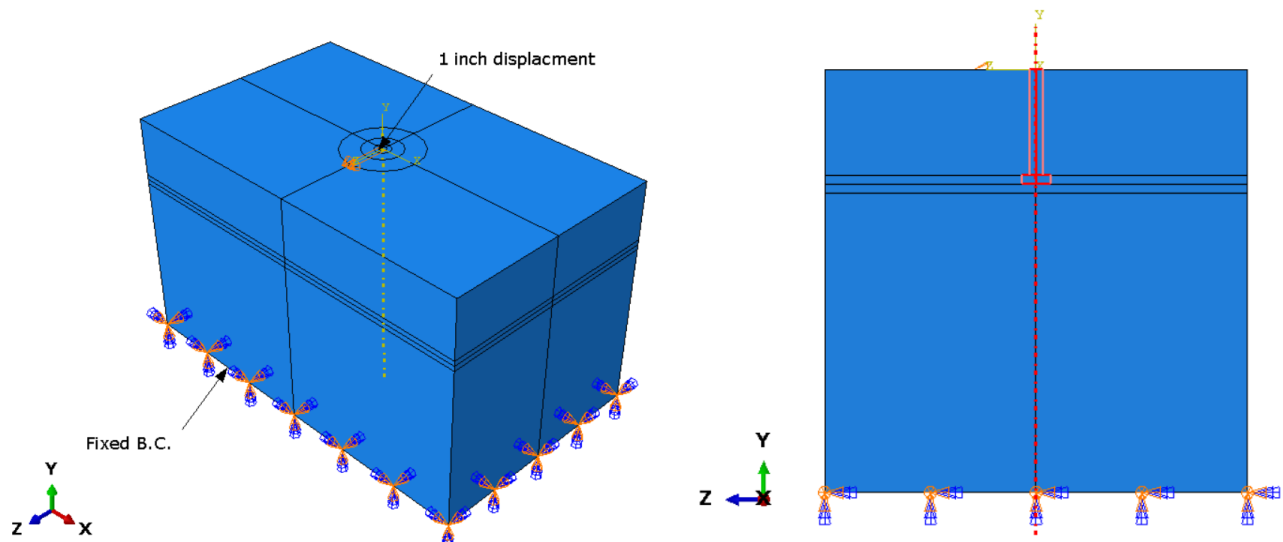


Figure 2.5 - Boundary Condition and Displacement Control (same for all models)

2.2.2 Model Properties

Concrete compressive and tensile damage properties are calculated using formulations provided by ABAQUS and calibrated in previous research (Zhang 2018). The values given in Table 8 have been adjusted for 4,000 psi concrete strength used in the models. The concrete damaged plasticity parameters are identical to properties from previous research (Zhang 2018) as follows:

- Dilation angle: 31°
- Eccentricity: 0
- Ratio of biaxial strength to uniaxial strength f_{b0}/f_{c0} : 1.16
- Ratio of the second stress invariant on tensile meridian K : 0.667
- Viscosity parameter: 0.0001

Table 2.1 - Concrete Compressive Damage Properties and Parameter adjusted for $f_c' = 4,000$ psi (Zhang 2018)

Concrete Compressive Behavior		Concrete Compressive Damage Behavior	
Yield Stress	Inelastic Strain	Damage Parameter	Inelastic Strain
4000	0.001945989	0	0
3821	0.002945989	0.466667556	0.001945989
3502	0.003945989	0.490564735	0.002945989
3183	0.004945989	0.533084678	0.003945989
2898	0.005945989	0.575662311	0.004945989
2654	0.006945989	0.61356392	0.005945989
2444	0.007945989	0.646195039	0.006945989
2265	0.008945989	0.674090928	0.007945989
2110	0.009945989	0.698000919	0.008945989
1976	0.010945989	0.71862303	0.009945989
1858	0.011945989	0.736542547	0.010945989
1754	0.012945989	0.752232837	0.011945989
1662	0.013945989	0.766072462	0.012945989
1580	0.014945989	0.778363974	0.013945989
1506	0.015945989	0.789350201	0.014945989
1439	0.016945989	0.799227314	0.015945989
1378	0.017945989	0.80815498	0.016945989
1323	0.018945989	0.816264167	0.017945989
1272	0.019945989	0.823663135	0.018945989
1225	0.020945989	0.830442047	0.019945989
1212	0.021235989	0.836676531	0.020945989

Table 2.2 - Concrete Tensile Damage Properties and Parameter adjusted for $f_c' = 4,000$ psi (Zhang 2018)

Concrete Tensile Behavior		Concrete Tensile Damage Behavior	
Yield Stress	Cracking Strain	Tension DMG	Inelastic Strain
474.341649	0	0	0
365.243070	0.000128421	0.437655012	0.00013
213.453742	0.000394737	0.671356825	0.00039
47.434165	0.001013158	0.926968183	0.00101

Only the elasticity of steel is included in the model parameters. Test data for plastic behavior was not available for materials similar to A449 steel. The following parameters were used in the steel material:

- Young's Modulus = 29,000 ksi
- Poisson's ratio = 0.30

After the models were completed, the stress in the anchor embedment was examined to verify the assumption of elasticity used for the material properties. The maximum stress was found to be generated in Model 2 with edge reinforcement and stirrups spaced at 4 in centers. The largest stress concentration was determined to be 94,230 psi. Using steel material properties for ASTM A449 steel, the yield stress for $\varnothing 3/4''$ rod is 92,000 psi and ultimate stress of 120,000 psi. The difference between the resultant stress and yield stress is as follows:

$$\text{Difference} = \left[\left(\frac{94,230}{92,000} \right) - 1 \right] \times 100 = 2.4\%$$

The difference between the yield stress and resultant stress is negligible, and therefore, the assumption of elasticity for steel is accurate.

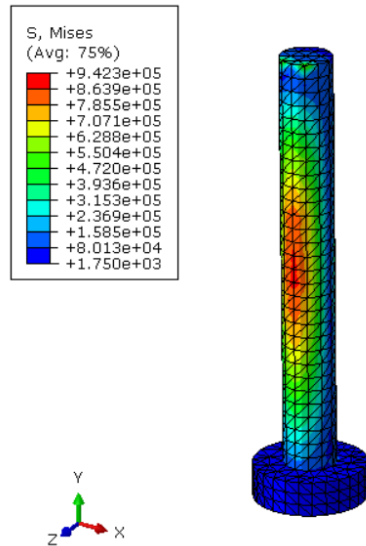


Figure 2.6 - Von Mises Stress for Steel Anchor (Model 2 results)

2.3 Finite Element Analysis Results

2.3.1 Control Model without Reinforcement (Model 1)

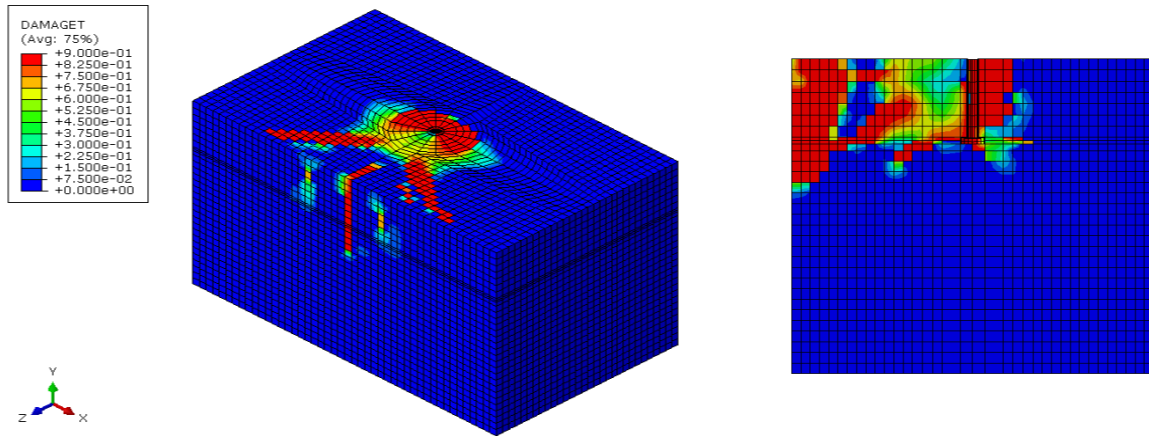


Figure 2.7 - Concrete Tensile Damage Parameter for Model 1

Figure 2.7 shows the resulting tensile damage due to the specified displacement. A maximum tensile damage value of 0.90 is achieved during this run. With the parameters adjusted for 4,000 psi concrete, the maximum calculated value for tensile damage is equal to 0.929 from Table 8. Percent difference between the calculated value and the analyzed value is calculated as: $0.929 / 0.90 = 1.03$. The difference of 3% can be attributed to the tension acting on the opposite side of the direction of the displacement. Since the tension damage parameter is not equal to 1.0 at these locations, there is still stress in those elements. The tensile stress on the backside of the anchor will counteract some of the forward displacement. This 3% difference is negligible for

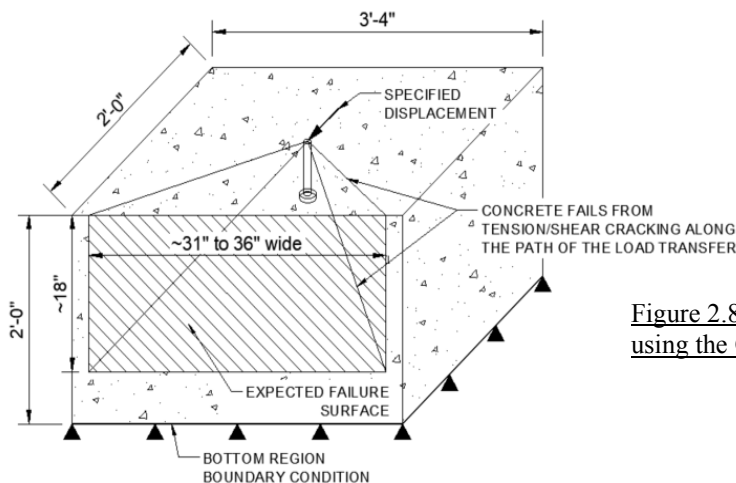


Figure 2.8 - Failure Surface predicted using the CCD Method

this study. The distribution of the tensile damage coincides with the anticipated failure surface predicted by the CCD method. During the original development of the CCD method test specimen had failure surface widths varying from $1.3c_{a1}$ to $1.5c_{a1}$ (See Figure 2.8).

Compressive damage also follows the expected distribution. The bearing force should be transferred to the concrete radially. The activated bearing according ACI 318-14 calculated values is $8d_a = 6$ in. The compressive damage parameter is at the maximum value over a majority of the depth of the embedment. Both the concrete damage and activated bearing indicate that the concrete compressive properties and model interactions are accurate (Figure 2.9).

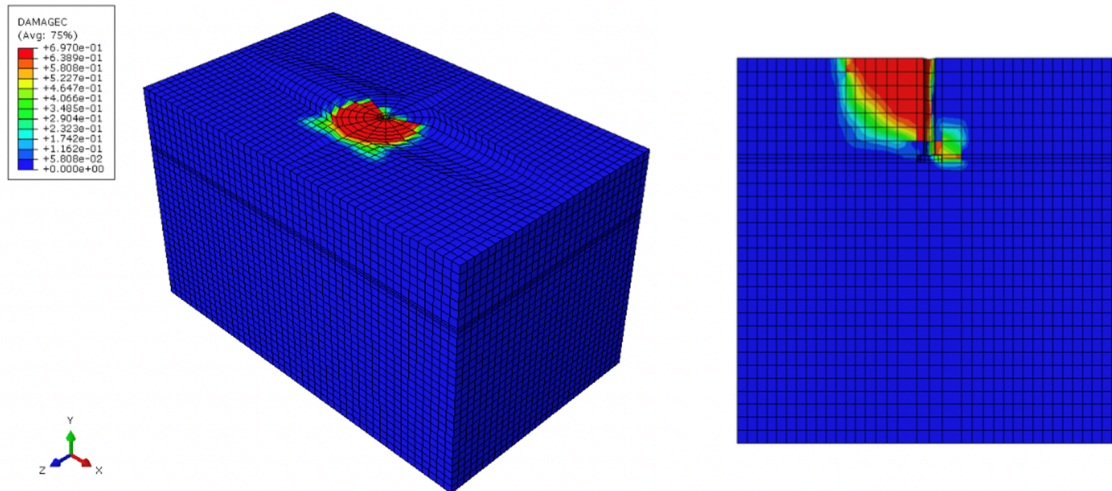


Figure 2.9 - Concrete Compressive Damage Parameter for Model 1

Evaluating the peak load of the control model against the calculation peak, the percent difference is calculated as:

- Peak Load = 29.9207 kips
- Calculated Value = 24.157 kips (See Appendix for calculation of anticipated failure load)
- Error % = $\left[1 - \left(\frac{24.157}{29.9207}\right)\right] \times 100 = 19.2\%$

Although 19.2% is not ideal, it appears that this is still within a reasonable range of that calculated value. Considering both the tensile and compressive damage and the failure surface shape, it is determined that this control model adequately represents the load-bearing response for plain concrete.

2.3.2 Control Model with Reinforcement 4in Spacing (Model 2, Figure 2.10)

The concrete tensile damage with stirrups follows a similar path as compared to the control model without reinforcement (See Figure 2.11). The difference between Model 1 and Model 2 is the stress concentrations in the stirrups embedded in the concrete.

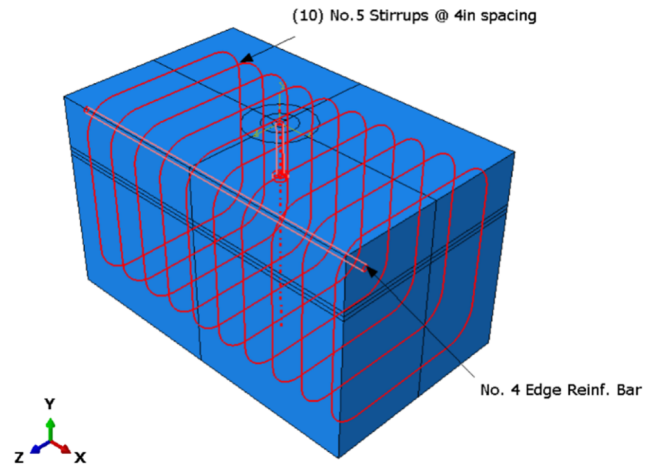


Figure 2.10 - Diagram of Model 2

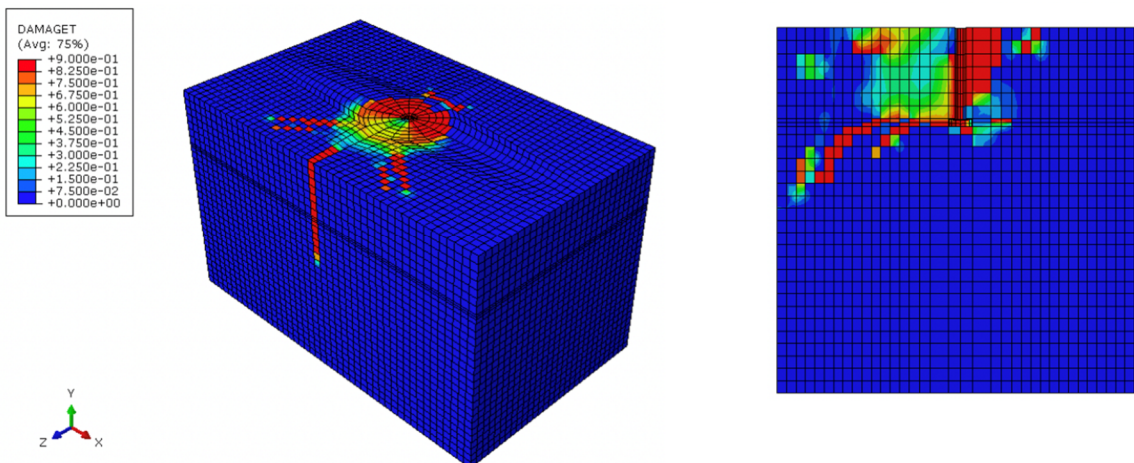


Figure 2.11 - Concrete Tensile Damage Parameter for Model 2

The increased peak load is due to the additional stress carried by the reinforcement. Stirrups closest to the anchor shown in Figure 2.12, resist the most stress. Peak value of 17,260 psi was observed during the control run. This stress is significantly lower than typical ultimate

stress of, $f_u = 40$ ksi or 60 ksi, for Grade 40 or Grade 60 respectively. This verifies the assumption that the steel reinforcement remains below the yield point and that the material properties are appropriate for this study. The peak load for the control reinforced model is equal to 32.8185 kips. Compared to the calculated value of 33.819 kips (See Appendix for calculation of anticipated failure load), the difference of 3% is negligible. The control model with reinforcement at 4in spacing accurately represents the anticipated load response.

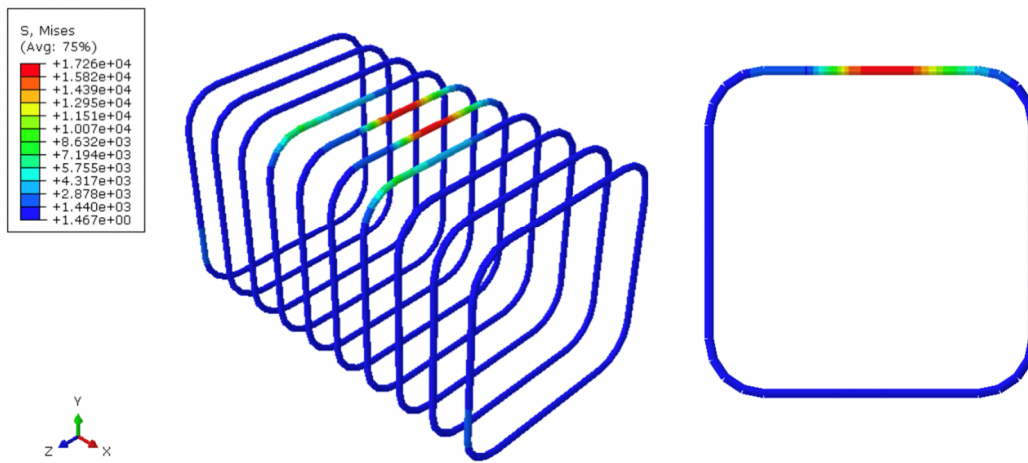


Figure 2.12 - Von Mises Stress in No. 5 Stirrups (left), Max stress on Single Stirrup (right) for Model 2

2.3.3 Experimental Model with Reinforcement 6in Spacing (Model 3, Figure 2.13)

In the first experimental model (Model 3), the stirrups are increased to a spacing of 6 in. This spacing does not conform to the confining requirement of 4 in spacing maximum. As the spacing increases, the reinforcement is farther away from the centerline of the anchor. This implies that the peak load of Model 3 with 6 in

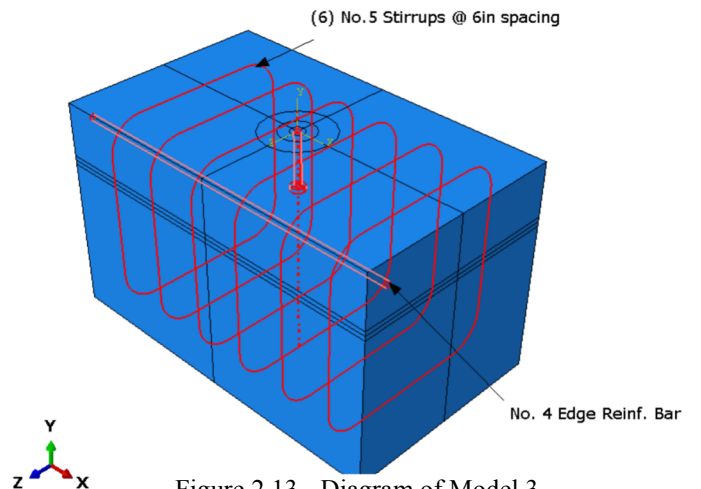


Figure 2.13 - Diagram of Model 3

spacing should be less than the peak load of the Model 2 with 4 in spacing. Figure 2.14 illustrates that the concrete tensile damage propagates to the anticipated failure surface as in the previous models.

Interestingly, comparison of the peak loads for Model 2 and Model 3 are almost equal, 32.8185 kips and 33.8719 kips respectively. The difference between peak loads of these models is equal to $(33.8719 / 32.8185) = 1.03$, a 3% increase in Model 3. The difference between the peak load and the calculated ACI 318-14 value is significant. Since 6 in spacing does not conform to the allowable spacing, a smaller modification factor is required. Comparing the calculated value from ACI 318-14 of 28.988 kips (See Appendix for anticipated failure load) to the FE model, the increase is calculated as follows:

$$\text{Diff \%} = \left[\left(\frac{33.8719}{28.988} \right) - 1 \right] \times 100 = 16.8\%$$

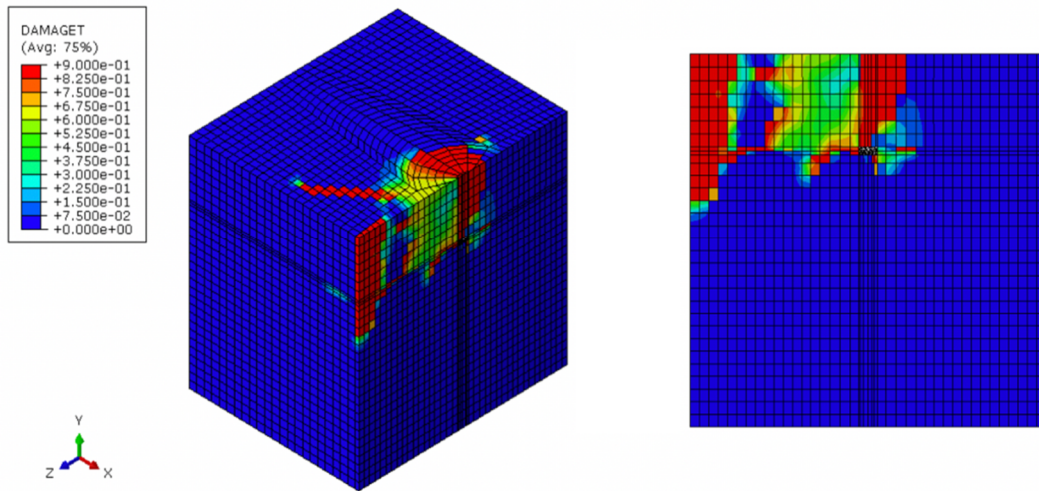


Figure 2.14 - Concrete Tensile Damage Parameter for Model 3

The maximum stress in the stirrup is equal to 13,900 psi and is located closer to the free edge of concrete (See Figure 2.15). Stress concentrating farther away from the anchor location is

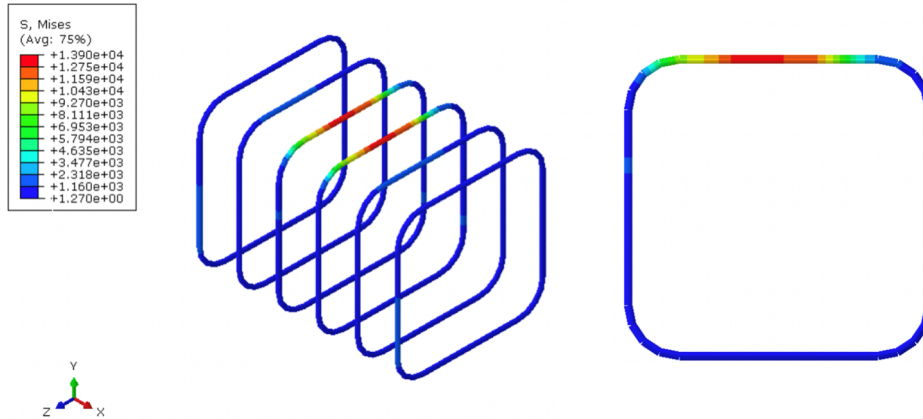


Figure 2.15 - Von Mises Stress in No. 5 Stirrups (left), Max stress on Single Stirrup (right) for Model 3 consistent with where the projected failure surface would theoretically intersect the reinforcement. Changing the spacing of the stirrups will also change the point at which the failure surface crosses the bar, resulting in different stress concentrations compared to Model 2.

2.3.4 Experimental Model with Reinforcement 8in Spacing (Model 4, Figure 2.16)

The second experimental model (Model 4), has stirrups spaced at 8 in apart. Again, this will not conform to the requirements for confining reinforcement and would be expected to have a peak load less than Model 2. The peak load value for Model 4 is equal to 33.459 kips, which is greater than Model 2, but less than Model 3 values.

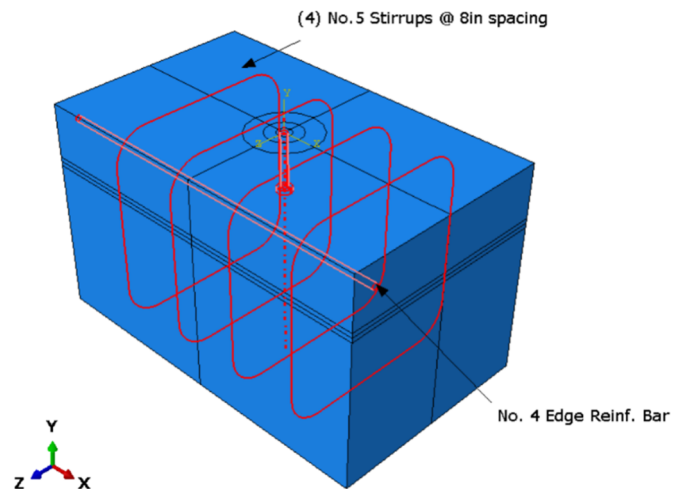


Figure 2.16 - Diagram of Model 4

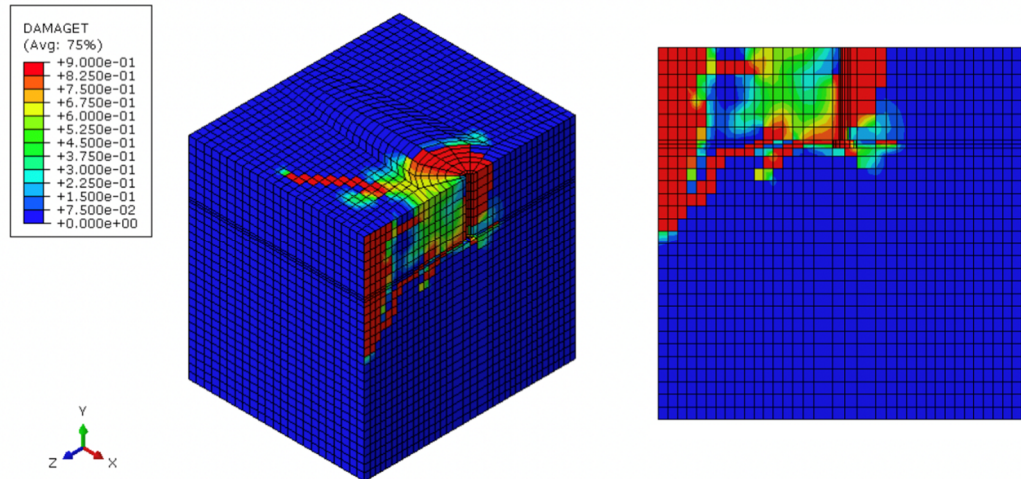


Figure 2.18 - Concrete Tensile Damage Parameter for Model 4

Similar to Model 3, the stress concentration in the stirrup is located further along the top horizontal bar. The maximum stress is equal to 14,930 psi (See Figure 2.18). This value is also between the upper and lower values of Model 2 and Model 3 respectively.

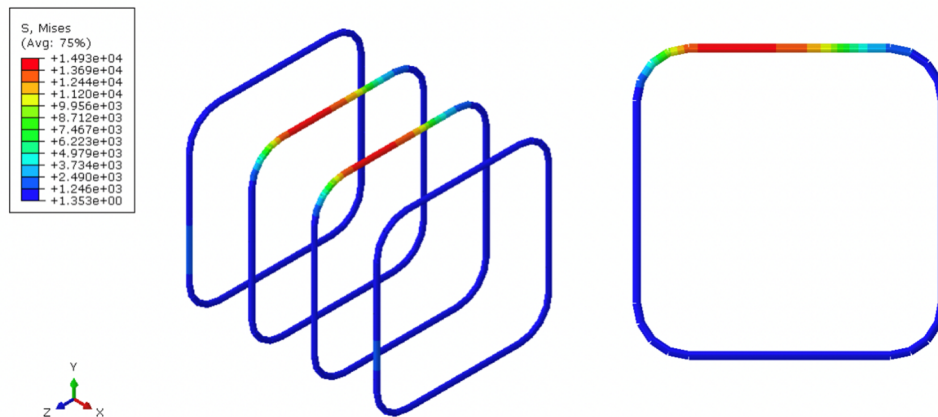


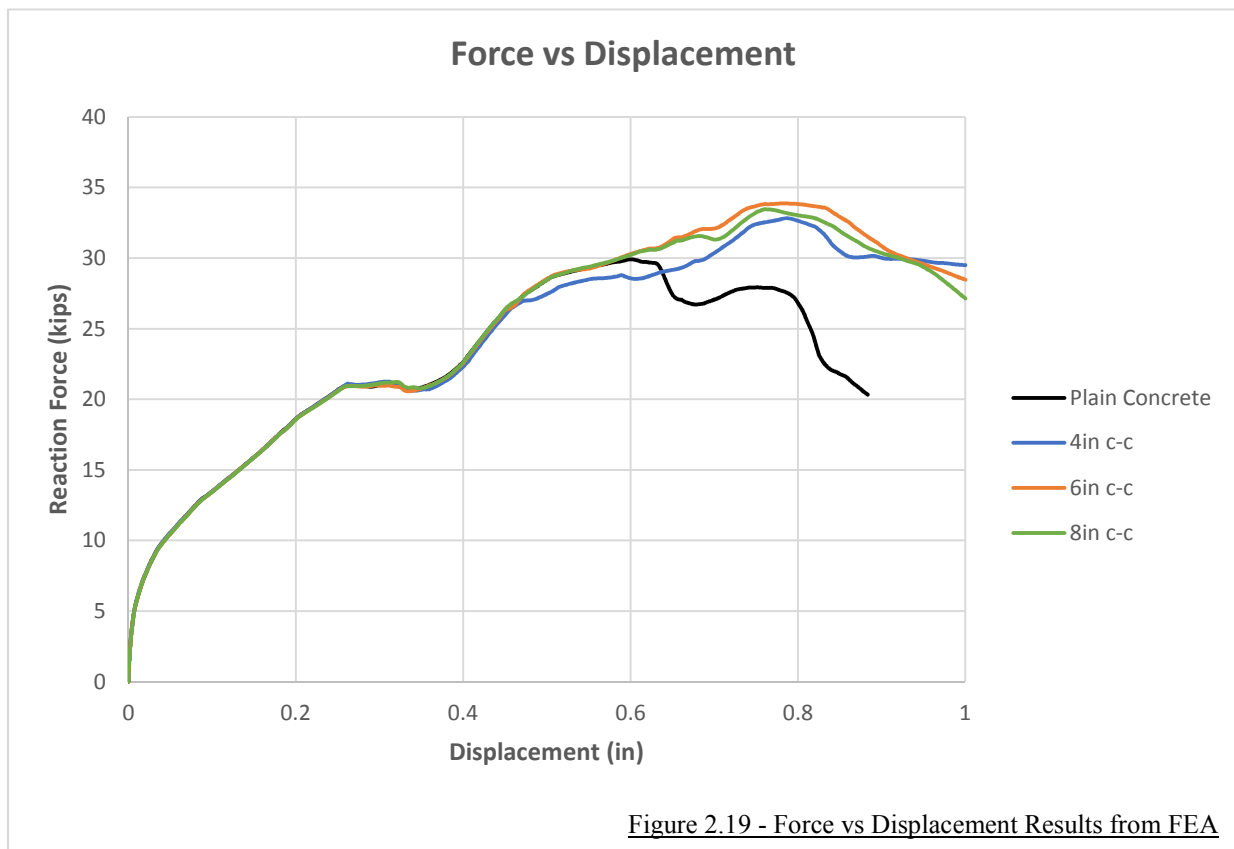
Figure 2.17 - Von Mises Stress in No. 5 Stirrups (left), Max stress on Single Stirrup (right) for Model 4

2.3.5 Force vs. Displacement Results

The summary of peak loads from FE model 1-4 and the anticipated failure load are as follows:

Table 2.3 - Summary of Peak Loads and Calculated anticipated Loads

Model # / Concrete Reinforcement	FE Model Peak Load (kips)	Anticipated Failure Load (kips)	Difference: FE vs. Anticipated (+ increase, - decrease)
Model 1 (Plain concrete)	29.9207	24.157	+19.2%
Model 2 (Edge + Stirrups at 4 in c-c)	32.8185	33.819	-3.0%
Model 3 (Edge + Stirrups at 6 in c-c)	33.8719	28.988	+16.8%
Model 4 (Edge + Stirrups at 8 in c-c)	33.4593	28.988	+15.4%



CHAPTER 3: CONCLUSION

3.1 Overall Conclusion

Based on these numerical studies it can be seen that the peak values for both of the control models are near the nominal strength that would be calculated with ACI 318-14 code. Being that the reinforced model with stirrups spaced at 4 in centers closely compared to the anticipated value, this implies that the other reinforced models adequately represents the actual load-bearing response. The load-displacement curve of the models using 6 in and 8 in spacing (Model 3&4, respectively) follow an identical path and give peak load values within 1.91% to 3.1% of the control reinforced model. Not only are the values very close to upper bound for the nominal strength, but these are significantly higher than the values calculated using ACI 318-14 code.

The initial hypothesis was that the 6 in or 8 in spacing would have a lesser peak load, but this was not the case. The test values for the two experimental models actually gave results higher than what was thought to be the maximum load. Model 3 gave the largest peak load, Model 4 in between that and Model 2.

Upon examination of the stirrups at each model, the location where the breakout failure surface occurs is very influential on the peak load. Another important factor is the stirrup's position relative to the anchor. As expected the development length will also play a role in the load resisted by each bar. Two main factors are in effect for each configuration 1) proximity to the anchor fastening and 2) development length inside and outside of the breakout surface. The following sections determines how each of these factors explain the numerical analysis results.

Model 2 - Stirrups at 4in spacing

- 1) These stirrups are in such close proximity to anchor, that these it does not require much strain or concrete damage for the steel to be mobilized. The largest displacement occurs near the anchor and concrete interface. The small sections of steel bar, although they have a much higher tensile strength compared to concrete, the stiffness is relatively small.
- 2) Bars placed close to the centerline of the anchor will have the most development length within the breakout surface. This is beneficial to the design.

Model 3 - Stirrups at 6in spacing

- 1) As the stirrups move further away from the centerline, more load must be dissipated into the structure before enough damage can occur to mobilize the reinforcement, some distance away. This is beneficial to increasing the capacity.
- 2) These bars still have a significant portion of the stirrup able to be developed inside the breakout surface, but will be limited on the allowable load.

Model 4 - Stirrups at 8in spacing

- 1) This position requires the most amount of load to be dissipated prior to mobilization of the steel.
- 2) These bars will have the least amount of development length available and will be limited on the total load carrying capacity.

This study was conducted using specific dimensions for the edge distance, concrete block, and stirrup spacing. Since only the elastic properties were used to model steel members in the control and experimental models, actual test data can be utilized to give a more accurate result for the steel load-bearing response. Including the plastic behavior or damage parameters of steel

will only increase the accuracy of the steel and concrete interaction. Future studies are strongly encouraged to include this information in FE models going forward.

Having an understanding how all the parameters involved can significantly influence the outcome of the study. The geometry of the model as well as boundary conditions will have a large impact on the results of individual studies. Keeping external factors, such as the boundary conditions, consistent across multiple studies will allow for more repeatability and consistency in the results. The stress concentration positions and magnitudes noted in these results, are dependent on this specific model and will change depending on the configuration. This study was design using an edge distance of 12 in that was chosen with the intent on providing enough distance to transfer load into the reinforcement and develop stress in the stirrups. To adequately evaluate whether the code is conservative, creating models to study individual variables is critical. Increasing stirrup spacing must be analyzed at shorter edge distances. Only by analyzing all the different configurations of anchor positions, stirrup spacing, and member size can a generalized conclusion be drawn.

3.1.1 Recommended Modification

Based solely on these tests, there is potential to include larger stirrup spacing for anchors under shear loading.

Current parameters:	$s \leq 4$ in [US]
	$s \leq 100$ mm [SI]
	Modification Factor, $\psi_c = 1.4$

Suggested parameters:	$s \leq 8$ in [US]
	$s \leq 200$ mm [SI]
	Modification Factor, $\psi_c = 1.4$

3.2 Field Application

Widening the range in which existing reinforcement can be used to resist shear loads will have huge cost savings benefits in the construction industry. A specific example would be in the construction of a high-rise building. It is common practice to use self-climbing wall forming systems in the concrete industry. This type of system incrementally works its way up the building while carrying workers, stored material, equipment, concrete placing boom, etc. In order to climb the building, anchors are set prior to each wall pour at specific elevations to provide connections points later on. Once the walls are cast, and have sufficient strength, raising the system can begin. Once lifted to the next elevation, the system is secured to the wall via the cast-in anchors.

This process is repeated at each level of the building, so efficiency is key. The structural engineer will specify the concrete strength based on code design requirements, not temporary construction conditions. But, the self-climbing system design requires a safe minimum concrete strength to support the tremendous vertical load applied by the self-climbing system. This means that the contractor's schedule is governed by how quickly the concrete cures. If concrete must one additional day per cycle, which could potentially add months to the duration of the project. With the additional strength that can be utilized from the existing reinforcement, the extra curing time could be eliminated entirely.

3.3 Future Studies

Further investigations need to be made into the other variables that are involved designing reinforcement. These parameters include, but are not limited to: influence of size effect, maximum stirrup spacing, stirrup bar diameter, and member size or geometry.

Current practice is to only include supplemental reinforcement that is placed within $0.5c_{a1}$ of the centerline of the anchor in the direction of the force. Reinforcement can be placed outside of $0.5c_{a1}$, but is still well within the range of the failure surface. Another area of focus would be testing whether the shear reinforcement is still effective with small edge distances. The reinforcement can only help resist the shear once some small cracking has occurred and the reinforcement is mobilized. Conversely, larger edge distances would have the room to allow for mobilization. This may lead to an over conservative design that with small edge distances, mobilization of the reinforcement may occur too late and be of benefit to the design. Another area for investigation is limitations of the bar size or reinforcement ratio used. Large diameter bars or increased quantities of rebar will be significantly stiffer than the concrete. With higher stiffness, the displacement or strain the concrete must also increase to mobilize a larger amount of steel. The continuation of this investigation through parametric studies is critical. Further studies will help expand and advance this field.

The construction industry is always moving and looking towards the future. Advances in technology are allowing engineers to design larger and more complex structures faster than ever before. Seeing that technology is going to continue to improve, engineers and researchers must also continue to find new ways to improve on our current methods. Research from years past must be evaluated and updated to keep from falling behind.

When certain fields within the industry exhaust all options and development begins to plateau, that's when we must re-evaluate what has been done in the past and update our old methods.

CHAPTER 4: REFERENCES

- ACI Committee 318, “*Building Code Requirements for Structural Concrete*” (ACI 318-08, -11, -14) and “*Commentary on Building Code Requirements for Structural Concrete*” (ACI 318R-08, -11, -14), American Concrete Institute, Detroit, 2008-2014.
- ACI Committee 349, “*Code Requirements for Nuclear Safety Related Concrete Structures*” (ACI 349-85, -97, -13), American Concrete Institute, Detroit, 1985-1997.
- ACI Committee 355, “*Guide for Design of Anchorage to Concrete: Examples Using ACI 318 Appendix D*”, Chapter 4. Example 8: Group of cast-in anchors in tension and shear with two free edges and supplemental reinforcement. American Concrete Institute, Detroit, 2011. Page 71-75\
- ACI Committee 446, “*Finite Element Analysis of Fracture in Concrete Structures*” (ACI 446.3R-97), American Concrete Institute, Detroit, 1997
- ACI Committee 446, “*Fracture Mechanics of Concrete: Concepts, Models and Determination of Material Properties*” (ACI 446.1R-91), American Concrete Institute, Detroit, 1991.
- “*Annual Steel Price Forecast.*” General Steel, 2019, gensteel.com/building-faqs/steel-building-prices/forecast.
- Bazant, Z. P., and Oh, B. H., “Crack Band Theory for Fracture of Concrete,” *Materials and Structures*, V. 16, No. 3, May-June 1983, pp. 155-177.
- Bazant, Z. P., “Size effect in Blunt Fracture: Concrete, Rock, Metal”. *Journal of Engineering Mechanics* ASCE, 1984, 110 (4), pp. 518 - 535.
- CEB, 1997, “Design of Fastenings in Concrete”, *Comite Euro-International du Beton* (CEB), Thomas Telford Services Ltd., London, UK, Jan.
- CEB, 1994, “Fastenings to Concrete and Masonry Structures, State of the Art Report,” *Comite Euro-International du Beton* (CEB), Bulletin No. 216, Thomas Telford Services Ltd., London, UK.
- Eligehausen, R., and Balogh, T., 1995, “Behavior of Fasteners Loaded in Tension in Cracked Reinforced Concrete,” *ACI Structural Journal*, V. 92, No. 3, May-June, pp. 365-379.
- Eligehausen, R.; Bouska, P.; Cervenka, V.; and Pukl, R., "Size Effect on the Concrete Failure Load of Anchor Bolts," *Fracture Mechanics of Concrete Structures*, Elsevier Applied Science, 1992, pp. 517-525.
- Eligehausen, R.; Mallee, R.; and Silva, J., 2006b, “*Anchorage in Concrete Construction*,” Ernst & Sohn (J. T. Wiley), Berlin, Germany, May, 380 pp.

- Eligehausen, R., and Ozbolt, J., "Size Effect in Anchorage Behaviour," Proceedings, European Conference on Fracture Mechanics, Fracture Behaviour and Design of Materials and Structures, Turin, Oct. 1991, pp. 17-44.
- FocusEconomics. "Steel Price (USA) | Historical Charts, Forecasts, & News." FocusEconomics | Economic Forecasts from the World's Leading Economists, 2019.
- Fuchs, W.; Eligehausen, R.; and Breen, J., 1995, "Concrete Capacity Design (CCD) Approach for Fastening to Concrete," *ACI Structural Journal*, V. 92, No. 1, Jan.-Feb. 1995, pp. 73-93. Also discussion, *ACI Structural Journal*, V. 92, No. 6, Nov.-Dec., pp. 787-802.
- Klingner, R.; Mendonca, J.; and Malik, J., 1982, "Effect of Reinforcing Details on the Shear Resistance of Anchor Bolts under Reversed Cyclic Loading," *ACI Journal Proceedings*, V. 79, No. 1, Jan.-Feb., pp. 3-12.
- Lee, N.; Park, K.; and Suh, Y., "Shear Behavior of Headed Anchors with Large Diameters and Deep Embedment," *ACI Structural Journal*, V. 108, No. 1, Jan.-Feb. 2010, pp. 34-41.
- Nilforoush, R.; Nilsson, M.; Elfgren, L.; Ozbolt, J.; Hofmann, J.; and Eligehausen, R., "Tensile Capacity of Anchor Bolts in Concrete: Influence of Member Thickness and Anchor's Head Size," *ACI Structural Journal*, V. 114, No. 6, Nov.-Dec. 2017.
- Ozbolt, J., "Smeared Fracture Finite Element Analysis—Theory and Examples," *International Symposium on Connections between Steel and Concrete*, R. Eligehausen, ed., RILEM Publication, Paris, France, 2001, pp. 609-624.
- Pearman, Dewey. "The Construction Workforce Shortage Is Expensive." Building Indiana, 26 Sept. 2018.
- Peterson D., Zhao, J., "Design of Anchor Reinforcement for Seismic Shear Loads," *ACI Structural Journal*, V 110, No 6 Feb. 2013, pp 53-62.
- Widianto; Owen, J.; and Patel, C., "Design of Anchor Reinforcement in Concrete Pedestals," *Proceedings of the 2010 Structures Congress*, Orlando, FL, 2010, pp. 2500-2511.
- Zhang, Yinglong, "Behavior of reinforced concrete walls with circular openings" (2018). *Graduate Theses and Dissertations*. 16702.<https://lib.dr.iastate.edu/etd/16702>

CHAPTER 5: APPENDIX A. HAND CALCULATIONS

Steel Anchor ASTM A449	Diameter : Shaft	Diameter : Head
Fu = 120,000 psi	3/4"	1-5/8"
Fy = 92,000		
Concrete	Compressive Strength, fc'	
	4,000 psi	

Calculate Shear Capacity of Steel Anchor using ACI 17.5.1

- The anchor detailed in the finite element model is assumed to be a stud and excludes the threads. Therefore, the shear ultimate strength will be determined by the gross area of the anchor shaft.

$$V_{sa} = A_{se,V} f_{uta} \quad (\text{ACI 17.5.1.2a}) \quad A_{se} = 0.442 \text{ in}^2$$

$$V_{sa} = (0.442)(120,000) = 53,040 \text{ lb}$$

Determine Critical Edge Distance for Concrete Breakout using ACI 17.5.2

- Determine critical edge distance based on the criteria for Concrete Breakout in Shear such that the fastening is limited by the strength of the steel anchor.

Nominal Shear Concrete Breakout Strength

$$V_{cb} = \frac{A_{vc}}{A_{vco}} \psi_{ed,V} \psi_{c,V} \psi_{h,V} V_b \quad (\text{ACI 17.5.2.1a})$$

- The concrete matrix used in the finite element model is designed such that the concrete breakout in shear capacity is not influenced by free edges. Therefore,

$$A_{vc} = A_{vco} \rightarrow \frac{A_{vc}}{A_{vco}} = 1.0$$

Modification Factor for Edge Distance (ACI 17.5.2.6)

$$\psi_{ed,V} = 1.0$$

Modification Factor for Cracked Concrete (ACI 17.5.2.7)

- Anchor is considered to be a location of cracked concrete. This will provide a lower predicted capacity, which results in a short critical edge distance.

$$\psi_{c,v} = 1.0$$

Modification Factor for Member Depth (ACI 17.5.2.8)

- The concrete matrix used in the finite element model is designed such that the concrete breakout in shear capacity is not influenced by the member depth.

$$\psi_{h,v} = 1.0$$

Determine Basic Concrete Breakout in Shear in terms of c_{a1} (ACI 17.5.2.2)

$$l_e = 8d_a = 8(0.75) = 6.0 \rightarrow \text{Use } l_e = 6\text{in}$$

$$V_b = \left[7 \left(\frac{l_e}{d_a} \right)^{0.2} \sqrt{d_a} \right] \lambda_a \sqrt{f'_c} (c_{a1})^{1.5} \text{ (ACI 17.5.2.2)}$$

$$l_e = 6\text{in} \quad d_a = 0.75 \quad \lambda_a = 1.0 \text{ (Norm. Wt)}$$

$$V_b = \left[7 \left(\frac{6.00}{0.75} \right)^{0.2} \sqrt{0.75} \right] 1.0 \sqrt{4,000} (c_{a1})^{1.5} = 581.13 c_{a1}^{1.5}$$

- Assume that anchor will be placed 12 in from the perpendicular direction of the free edge of concrete.

$$V_b = 581.13(12)^{1.5} = 24,157 \text{ lb}$$

Determine anticipated load for Concrete Breakout in Shear @ 12 in edge distance

$$V_{cb} = \frac{A_{vc}}{A_{vco}} \psi_{ed,v} \psi_{c,v} \psi_{h,v} V_b \rightarrow V_{sa} = (1.0)(1.0)(1.0)(24,157) = 24,157 \text{ lb}$$

- 24,157 lb is the anticipated mean load at which plain concrete is predicted to fail.

$$24,157 \text{ lb} \leq 53,040 \text{ lb} \rightarrow \text{Concrete governs over anchor shear capacity}$$

Determine Concrete Model Geometry based on critical edge distance, c_{a1}

$c_{a1} = 12\text{in}$ (Assumed for the purposes of this study)

- Design c_{a2} and member depth, h_a , such that projected failure surface is not influenced by free edges. Thereby, validating the assumptions above for the modification factors for edge distance and member depth.

$$c_{a2(\text{Min})} = 1.5c_{a1} \times 2 = 1.5(12) \times 2 = 36\text{in} \rightarrow \text{Use } 40\text{in}$$

$$h_{a(\text{Min})} = 1.5c_{a1} = 1.5(12) = 18\text{in} \rightarrow \text{Use } 24\text{in}$$

Calculate Concrete Breakout in Shear with Supplemental Reinforcement

- Assume edge reinforcement and stirrups spaced at 4 in centers

According to ACI 318-14, Ch 17.5.2

Condition “A” per ACI 17.3.3

All parameters are calculated similar to “Plain concrete” condition with the exception of the following:

Modification Factor for Uncracked/Cracked Concrete (ACI 17.5.2.7)

Anchor is considered to be in a region of cracked concrete. Reinforcement is provided by No. 4 bar between the anchor and the edge, and enclosed within stirrups spaced at 4 in centers.

$$\psi_{c,v} = 1.4 \text{ (cracked concrete at service loads with supplemental reinforcement)}$$

Calculate Concrete Breakout in Shear

$$V_{cb} = \frac{648}{648} (1.0)(1.4)(1.0)(24,157) = 33,819 \text{ lb}$$

- 33,819 lb is the anticipated mean load at which reinforced concrete is predicted to fail.

Calculate Concrete Breakout in Shear with Supplemental Reinforcement

- Assume edge reinforcement only.

According to ACI 318-14, Ch 17.5.2

Condition “A” per ACI 17.3.3

All parameters are calculated similar to “Plain concrete” condition with the exception of the following:

Modification Factor for Uncracked/Cracked Concrete (ACI 17.5.2.7)

Anchor is considered to be in a region of cracked concrete. Reinforcement is provided by No. 4 bar between the anchor and the edge.

$\psi_{c,v} = 1.2$ (cracked concrete at service loads with edge reinforcement) .

Calculate Concrete Breakout in Shear

$$V_{cb} = \frac{648}{648} (1.0)(1.2)(1.0)(24,157) = 28,988 \text{ lb}$$

- 28,988 lb is the anticipated mean load at which edge reinforced concrete is predicted to fail.